IMPROVING SUSPENSION IN A QUARTER CAR MODEL TEST FROM AERO POST RIG ANALYSIS: PERFORMANCE INDEX

AUTHORS:

Timoteo Briet Blanes

AERODYNAMICS RESEARCH GROUP

ABSTRACT

The performance of an F1 race car is greatly influenced by its aerodynamics. Race teams try to improve the vehicle performance by aiming for more levels of downforce. A huge amount of time is spent in wind tunnel and track testing. Typical wind tunnel testing is carried out in steady aerodynamic conditions and with car static configurations. However, the ride heights of a car are continuously changing in a race track because of many factors.

These are, for example, the roughness and undulations of the track, braking, accelerations, direction changes, aerodynamic load variations due to varying air speed and others. These factors may induce movements on suspensions components (sprung and unsprung masses) at different frequencies and may cause aerodynamic fluctuations that vary tires grip. When the frequency of the movement of a race car is high enough the steady aerodynamic condition and the car static configurations are not fulfilled. Then, transient effects appear and the dynamics of the system changes: heave, pitch and roll transient movements of the sprung mass affect both downforce and center of pressure position. The suspension system have to cope with them, but in order for the suspension to be effective, unsteady aerodynamics must be considered.

The main objective is to model the effects of unsteady aerodynamics and know really the car dynamic, with the aim of optimizing the suspension performance, improving tire grip and finally reducing lap times.

KEYWORDS

Transitory, transient aerodynamic, CFD, damper, spring, performance index, suspension improve, lissajous, aerodynamic no lineal, aero map, race car, down force, transitory aerodynamic, car suspension, suspension, sprung mass, unsprung mass, vehicle dynamic, lap time.

NOMENCLATURE

Am = Amplitude vibration (m).
f = Frequency vibration (Hz).
t = Time (s).
U_∞ = Air velocity (m/s).
m_s = Sprung Mass (kg).
m_u = Unsprung Mass (kg).
K_s = Spring constant sprung mass (N/m).
K_u = Spring constant unsprung mass (N/m).
C_s = Damper constant sprung mass (N/ms).
C_u = Damper constant unsprung mass (N/ms).
Y = Height in axis vertical (m).
f_{aero} = TF = Wing Transfer Function Aerodynamic.
I = Input Signal.
O = Output signal.
θ = Phase Angle.
dB = Decibels.
N = Number of points.
T = Signal vibration period (s).
Tp = Delay between two vibrations (s).
PI = Performance Index.
Setup = Set of car suspension values, masses and dimensions.

INTRODUCTION

There are many studies about the aero static or without aero values; perhaps, there are some studies with transient aero in vehicles and they effects; some papers about, work with CFD techniques:

In [1], study the change downforce depending on the height above ground; in this case, it works on a simple profile placed close to the ground, where the ground effect is very important. In [3], study the influence on parts of a car vibrations caused by transient aerodynamics. In paper [4], the downforce generated by a simple motion profile heave and pitch for different frequencies is analyzed; this study was performed from CFD studies and wind tunnel tests; the results are compared with model results Theodorsen. In paper [19], study the downforce variation for profile (Naca 0012) between -5º and 13º in wind tunnel; the aerodynamic values are static. In [30], study the downforce with aerodynamic transient of Ahmed Body, front pitch position. In [14], analyze the effects of transient aerodynamic forces in car stability are studied. Joint simulations CFD and test in wind tunnels, show that the aerodynamic effect is transient and reduces the pitching resonance frequency of the sprung mass vehicle. One of the phenomena studied is the "porpoising" effect that makes the vehicle suffer pitch oscillations of great amplitude, which affect vehicle dynamics in a nonlinear way.

Also, there are studies about active suspension in cars or control of flight in planes, in order to improve the comfort of passengers or vehicle behavior; for that, define and analyze some performances index (PI):

In [5], a magneto-rheological suspension is applied to improve the suspension of a bicycle model of a vehicle; no aerodynamic values are used and PI is defined to achieve optimization. In [18], study the influence of transient aerodynamics in the fast and high amplitude of small wing movement is studied. The idea is that the aerodynamic models used for flight control, based on assumptions of quasi-static conditions are valid for conventional aircraft. Also, it examines the aerodynamic effects of an inverted wing ground effect performing a vertical ("heave") sinusoidal movement at different frequencies. In [22], improve behavior car from active control surfaces in order to variate the ride control in sport cars; define a new PI. In [23], define a PI for improving behavior car from active and semiactive suspension. In [21], study a PI for improving car passenger suspension and road holding. In [20], study the quarter car optimization from active and semiactive suspension under random road excitation; define PI. In [24] and [26], analyze the suspension improve from inerters and hydraulic actuators; analyze the PI. In [27], analyze the comfort with the aerodynamic controlled surfaces in unsprung mass. In paper [7], analyze the influence of transient aerodynamics in the fast and high amplitude of small wing movement is studied. The idea is that the aerodynamic models used for flight control, based on assumptions of quasi-static conditions are valid for conventional aircraft. In [16], analyze the effect of tire damping on the performance of vibration absorbers in an active suspension; use Pi and transfer functions. In [11], study the PI for damper variable in active suspension; 1 Hz to 100 Hz and quarter car model. In [17], analyze the influence of transient aerodynamics in the fast and high amplitude of small wing movement is studied. The idea is that the aerodynamic models used for flight control, based on assumptions of quasi-static conditions are valid for conventional aircraft. Also, it examines the aerodynamic effects of an inverted wing ground effect performing a vertical ("heave") sinusoidal movement at different frequencies. In [10], analyze the PI of a car with suspension active using quarter car model for different road profile. In [9], study the suspension active applied in race cars. In [15], analyze one new PI for improving dynamic vehicle.

Another's studies, work about analysis post rig (a post test rig, produce a known input signal or excitation and compare this signal with the output signal may be the movement of the sprung and unsprung mass; by this comparison, it is possible to optimize the damper) or lap time, applied to cars; there are not aero transitory or aerodynamic values in general:

In [8], study 8 post rig 8 analysis without aero; the goal is improve the damper for race cars. In [12], analyze the PI in a half car model with engine, differential, etc. (full lap time). This study is without aerodynamic values; in [28], improve the dynamic vehicle analyzing PI without aerodynamic values.

In [25], analyze the influence of mass added in heave vibration on object in water. Finally in [29] and [34], improve the vehicle behavior from inters dampers (for that, define a PI) and stiffness or pressure wheel and damper.

The structure and parts of this paper are:

Point 1: The geometry used for the CFD tests described; is vibrated up - down geometry at different frequencies and amplitudes, calculating the downforce that the profile generated against the vertical position. The data is displayed as Lissajous curves. That is the first step for aiming to know and understand what happens to the downforce if the wing vibrates.

Point 2: Is explained the existing problem with nonlinear dynamics and method to solve it: generating a transfer function (TF) from a number of cycles or periods using as input data the tests in point 1 is proposed. That TF will be the aero – function for using in this paper.

Point 3: It described the two models will be used for test the new procedure created in this paper: the quarter car model without the intervention of aerodynamic forces and quarter car model in the presence of TF aerodynamic generated in point 2.

Point 4: The basic objective is to compare real data with data obtained from the procedure established in this paper; For this, a "real" test is created from a CFD simulation; this simulation CFD tested any vibration on the quarter car defined in point 3.

Point 5: In this essential point, it compare data from point 3 against data point 4; with that, will be possible to validate the new procedure of this paper.

Point 6: To know whether or not improved suspension parameters, a set of values defined whose mission is to quantify the possible improvement; the first value quantifies the Bode plot, the second quantized value variations in height (sprung and unsprung mass) and the third value takes into account the tire contact patch.

Point 7: Finally, as mentioned objective is to optimize the setup of a car; for it and to validate the procedure established in this paper, the damper of the suspension of the quarter car model of point 3 is optimized, obtaining different improved values, depending if it want to improve the movement of the sprung mass or unsprung mass.

Point 8 and 9: Conclusions, future directions and references.

1. COMPUTATIONAL SIMULATION
1.1. TEST GEOMETRY

The geometry (typical in wings cars competition but also in sport cars) to study combine two profiles Naca 4612 (Fig.1) composite:

The measures are:

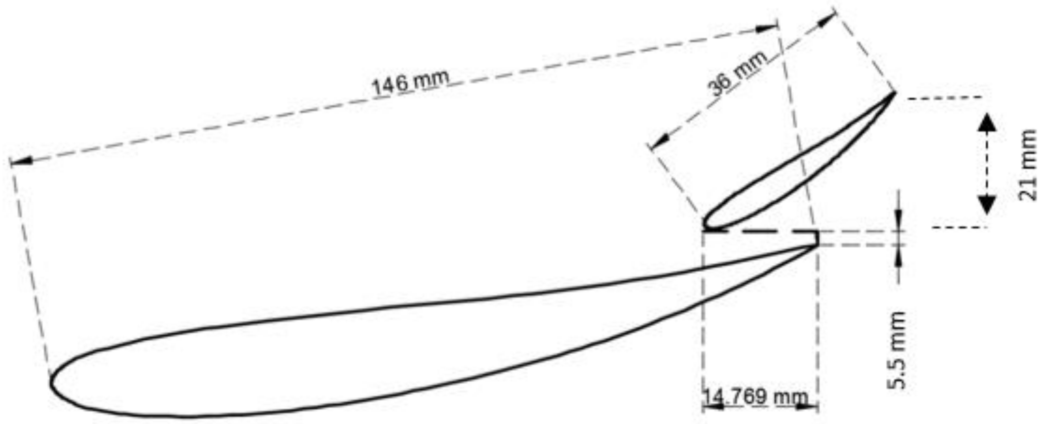

Fig.1 Measures composition Profiles Naca.

The incidence angle (5 degrees) of the geometry tested is (Fig.2); this angle is typical for cars low downforce:

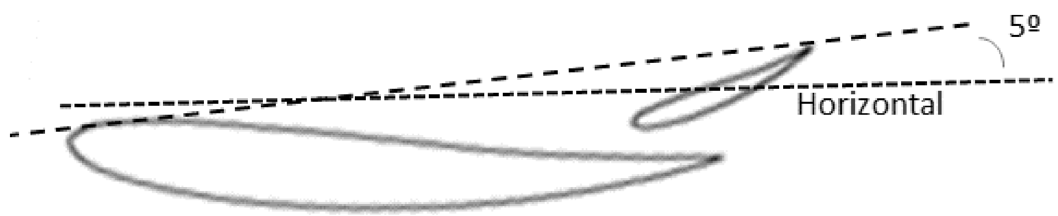

Fig.2: Incidence angle geometry.

The span (perpendicular to profile) is 1500 mm (Fig.3):

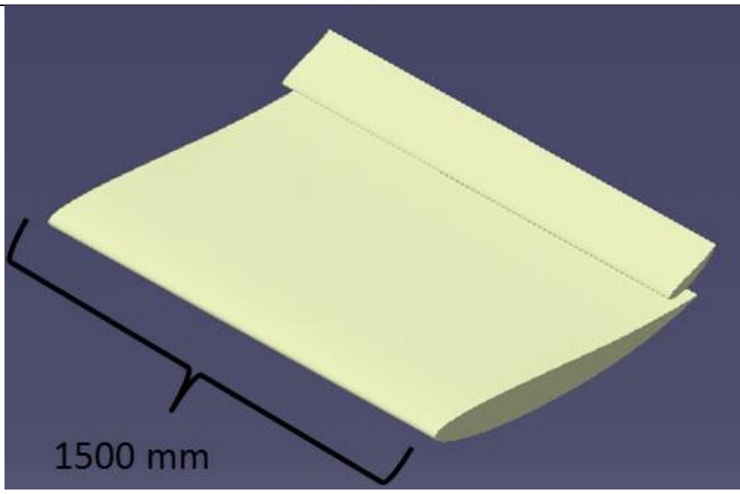

Fig.3: Span wing

1.2. SIMULATION CONDITIONS

First fixed geometry allowed to air flow stabilizes; this happens by 0.11 seconds; once the flow has stabilized, the geometry is vibrated up and down (direction "y"), perpendicular flow direction.

The movement can vary in amplitude (Am in "m") and frequency (f in "Hz") (Eq.1):

$$y(t) = Am \cdot \sin\left(f \cdot (t - 0.11)\right)$$

Eq.1: Amplitude input signal.

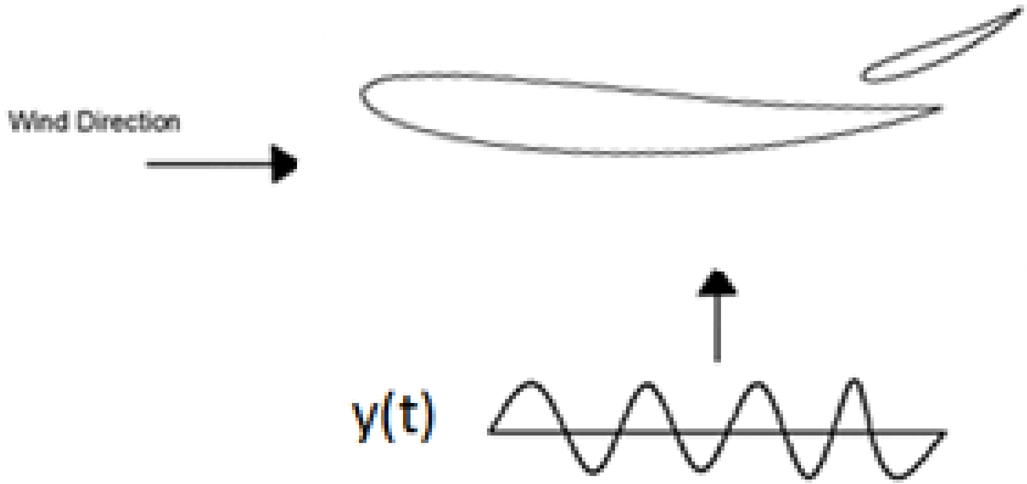

The frequencies chosen for the simulations are:1Hz, 3Hz, 5Hz, 8Hz, 10Hz, 11Hz, 13Hz,15Hz, 18Hz, 20Hz, 23Hz, 25Hz, 28Hz, 30Hz, 33Hz, 35Hz, 38Hz, 40Hz, 66Hz, 80Hz, 100Hz, 500Hz and 800Hz, with allows for a complete study of the behavior of the profile in a large frequency range and specially all the most important frequencies in relation to the vibrations of a vehicle (not covered so far in the literature);); the amplitude has been chosen from the next Table 1 for all frequencies:

Hz	Am (mm)
1	20,00000
3	15,00000
5	12,00000
8	6,00000
10	3,00000
11	3,00000
13	3,00000
15	3,00000
18	3,00000
20	2,00000
23	2,00000

Hz	Am (mm)
25,00000	2,00000
28,00000	2,00000
30,00000	2,00000
33,00000	2,00000
35,00000	2,00000
38,00000	1,00000
40,00000	1,00000
66,00000	1,00000
80,00000	0,50000
100,00000	0,40000
500,00000	0,20000
800,00000	0,1

Table 1: Amplitude against frequencies.

The software CFD used is Star CCM+ V.9.02-007 (Company: CD-Adapco), resolving the Navier Stokess equations [33]; the values of the simulation are (mesh and programation):

About the mesh (Fig.4 and Fig.5):

Mesh model = Morphing mesh; Growth Rate = 1.01 (same mesh density in all wind tunnel); Base size = 0.1m; Size minimum in wings = 0.0005m; Size target in wings = 0.001m; Number layers in boundary layer = 10; Stretching factor boundary layer = 1.1 (thickness proportion between two layers together); Thickness first layer boundary layer = $6*10^{-6}$m; Courant Friedrich Levy (CFL) number = 1; all these values providing the best possible precision [32].

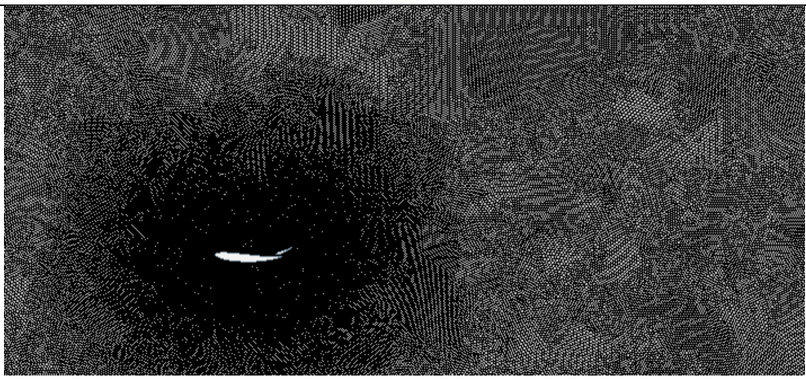

Fig.4: General mesh.

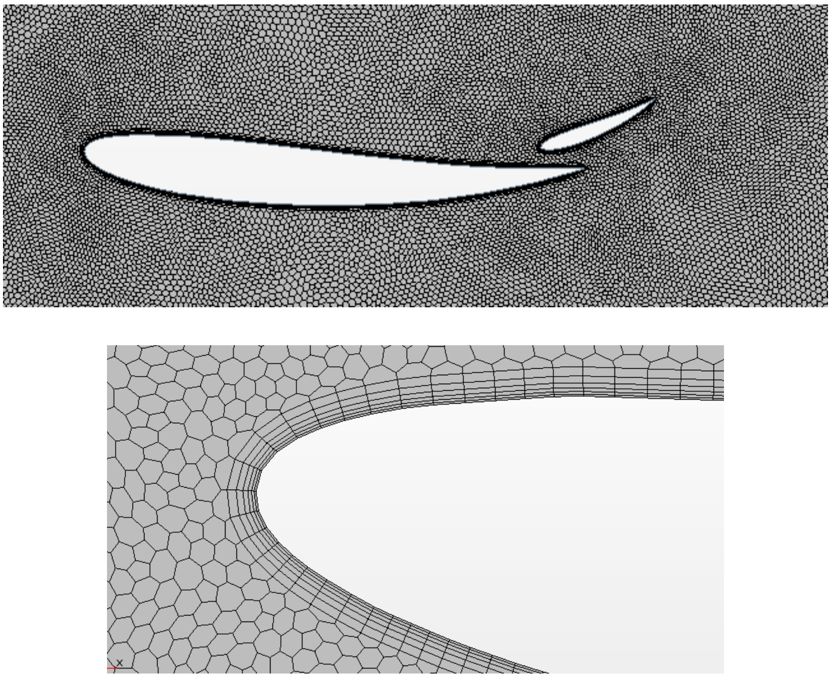

Fig.5: Detail mesh with boundary layer.

About the programation: U_∞ = 50 m/s (reference speed as medium speed, in race cars); Temperature air = 20ºC; Atmospheric pressure = 1012 mbar; Phisics models equations = Navier Stokess equations; Turbulence model = K-Epsilon [31].

1.3. RESULTS

In order to show some results (Fig.6, 7, 8, 9, 10, 11 and 12), it can plot the downforce against the position of the first period (up – down); if going up geometry shown in red, else in blue. This plot is named Lissajous curve.

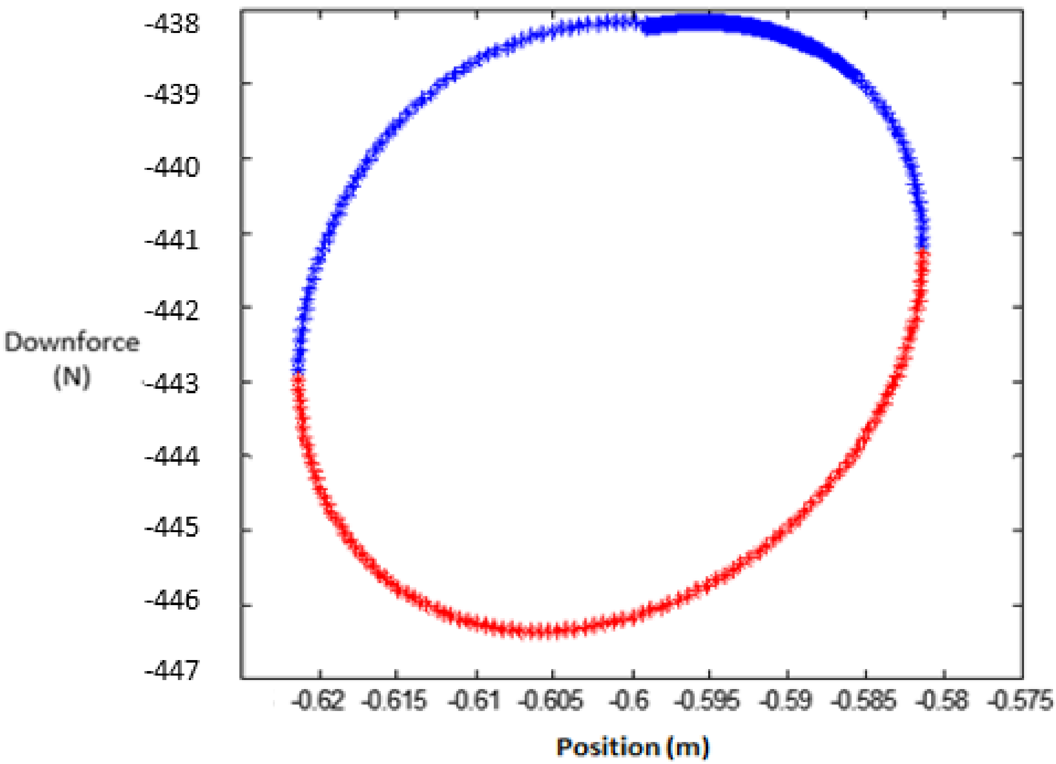

Fig.6: 1Hz

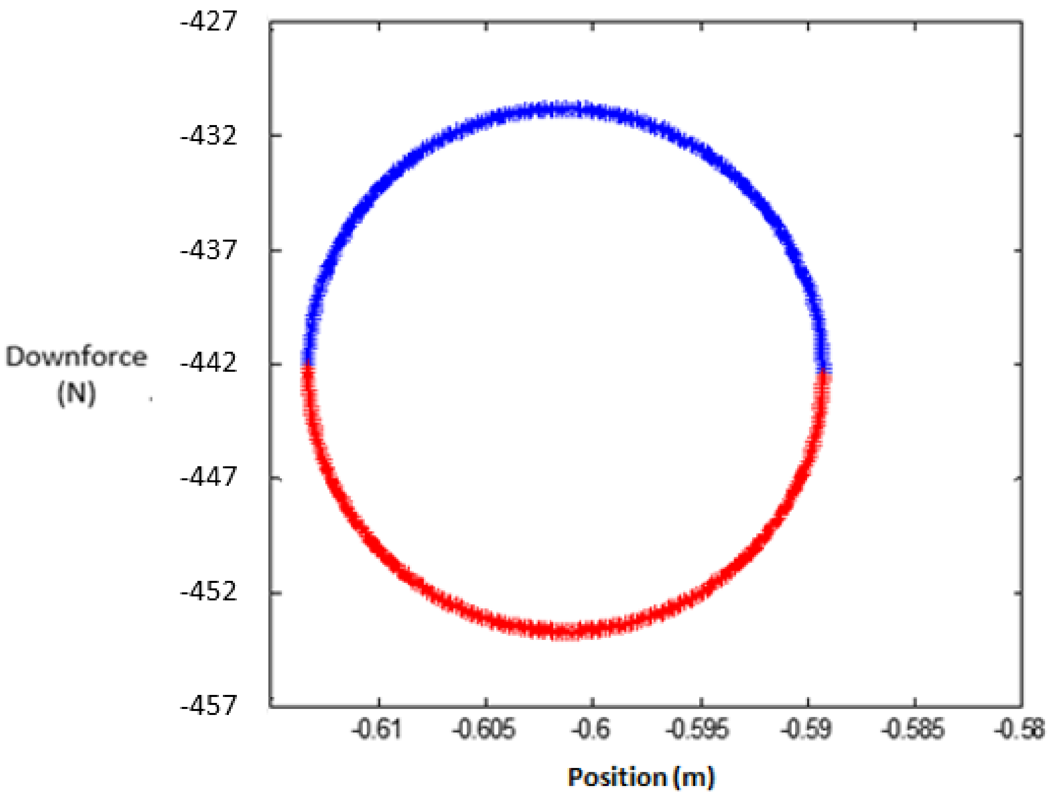

Fig.7: 5Hz

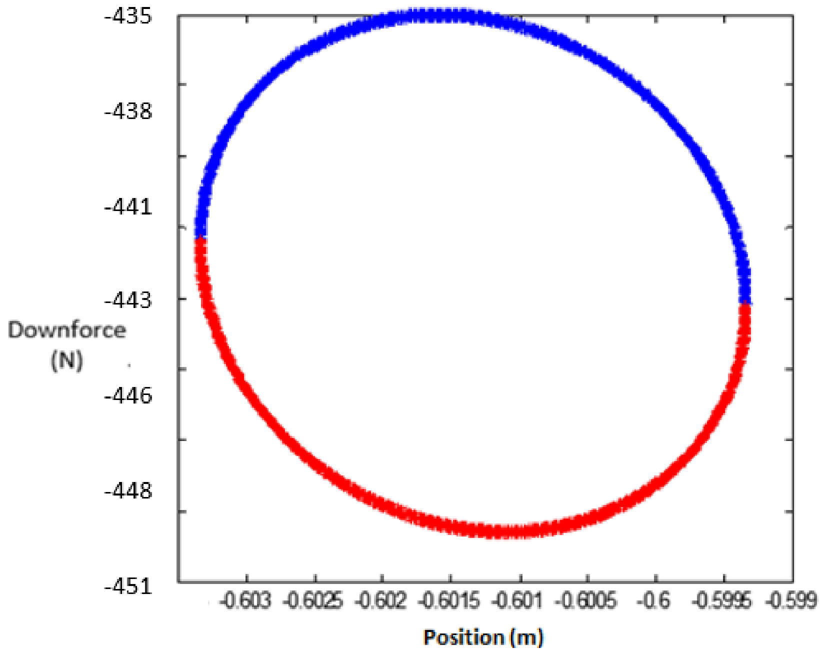

Fig.8: 25Hz

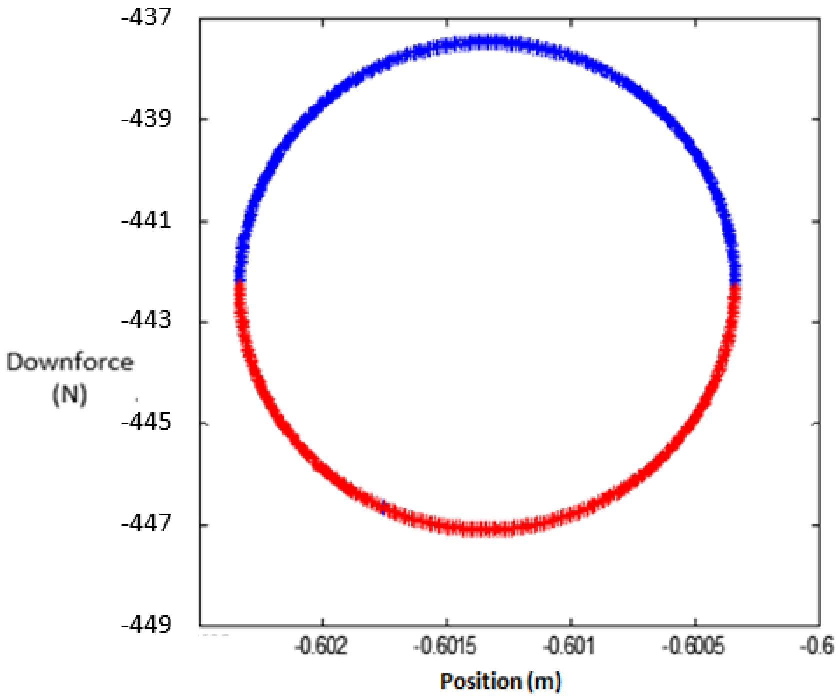

Fig.9: 38Hz

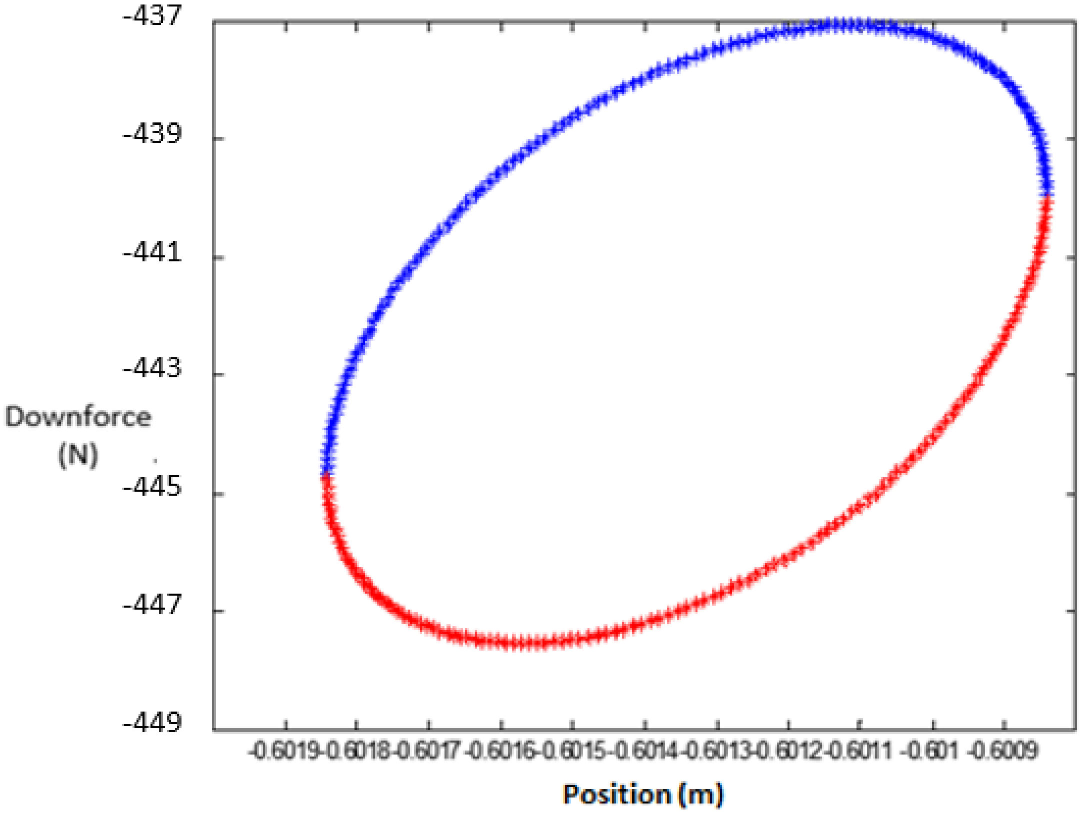

Fig.10: 80Hz

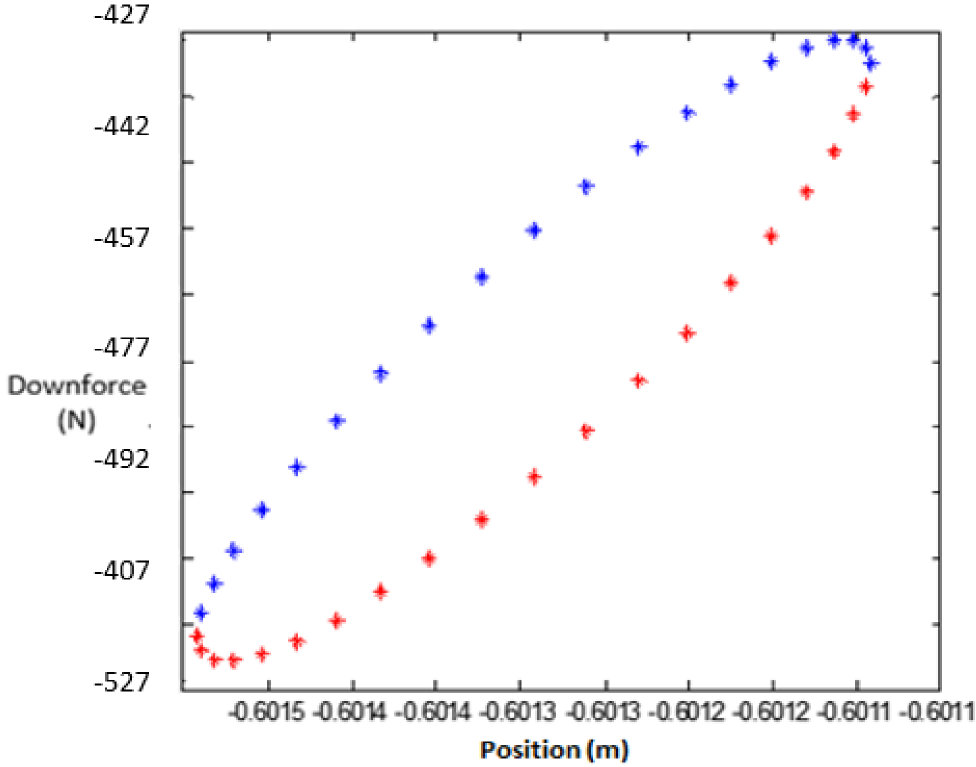

Fig.11: 500Hz

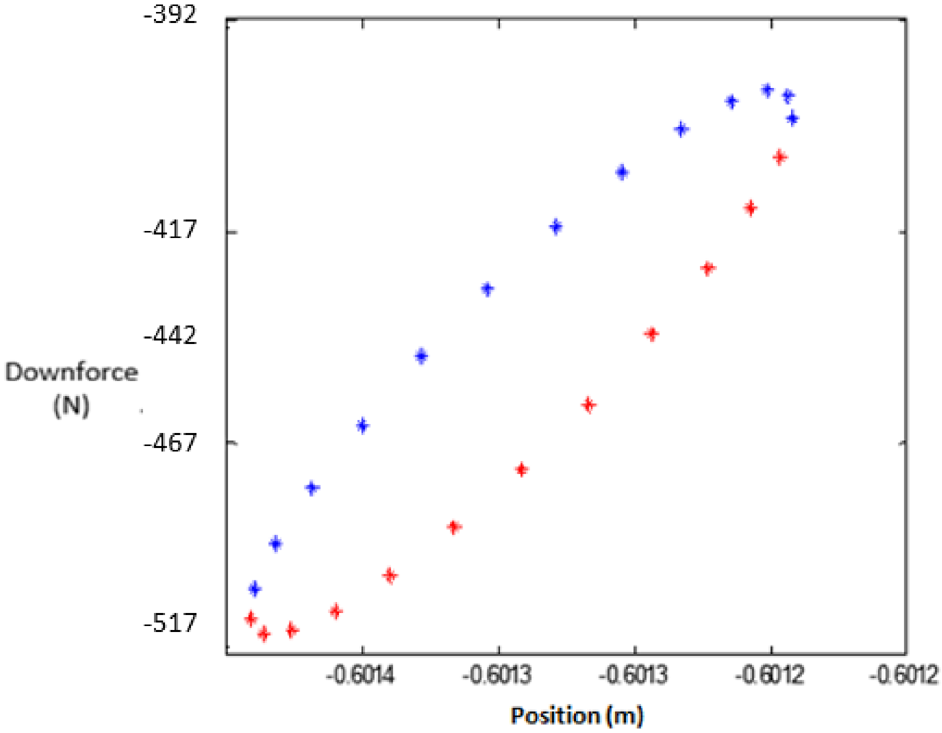

Fig.12: 800Hz

It can see that the downforce quantity is not symmetrical up-down, so the profile is not symmetrical too.

1.4. GEOMETRY LISSAJOUS STUDY

In order to know what is Lissajous curves variation, in function of input amplitude and frequencies, it show the next curves:

Fig.13-33Hz Frequency: Amplitudes: 1mm, 2mm, 4mm and 6mm, Fig.14-66Hz Frequency: Amplitudes: 1mm, 2mm, 4mm and 6mm , Fig.15-99Hz Frequency: Amplitudes: 1mm, 2mm, 4mm and 6mm, Fig.16-1mm Amplitude: 33Hz, 66Hz and 99Hz , Fig,17-2mm Amplitude: 33Hz, 66Hz and 99Hz, Fig.18-4mm Amplitude: 33Hz, 66Hz and 99Hz, Fig.19-6mm Amplitude: 33Hz, 66Hz and 99Hz:

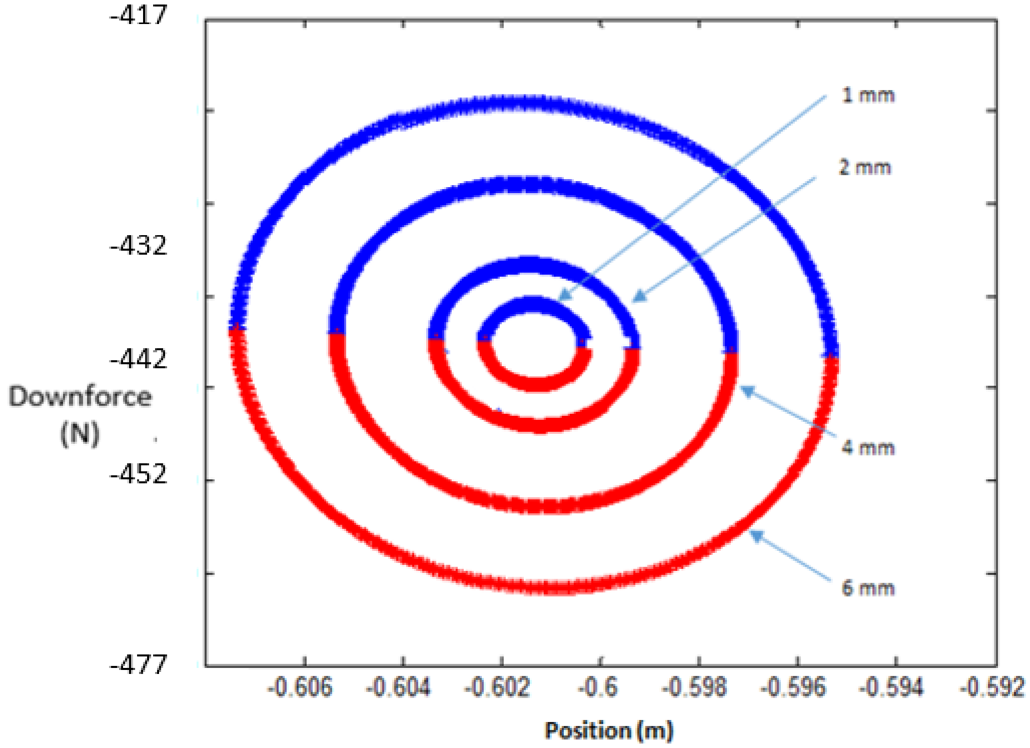

Fig.13: 33Hz: Amplitudes: 1mm, 2mm, 4mm and 6mm.

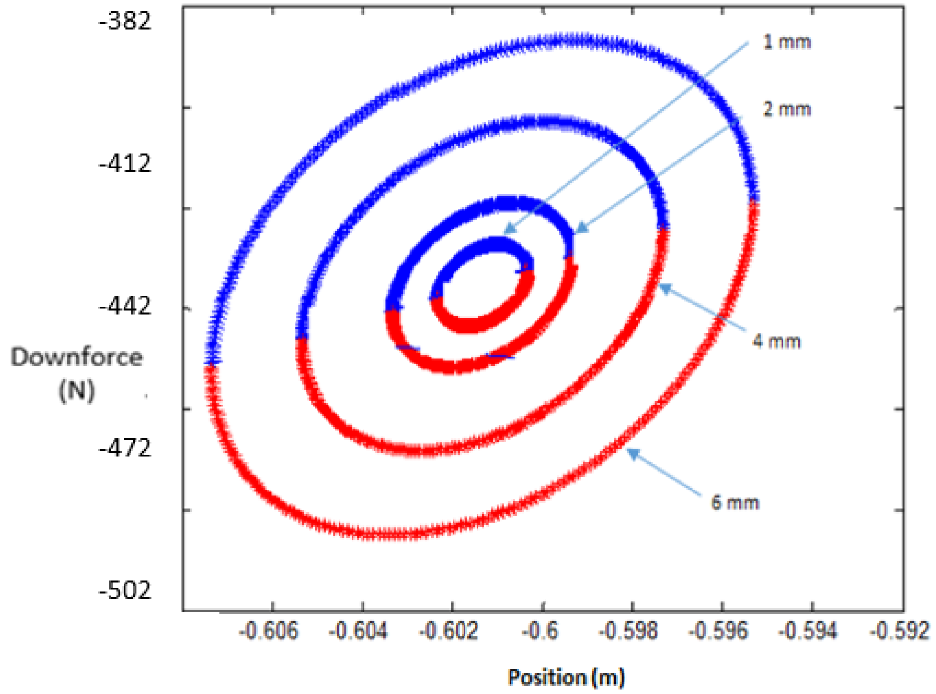

Fig.14: 66Hz: Amplitudes: 1mm, 2mm, 4mm and 6mm.

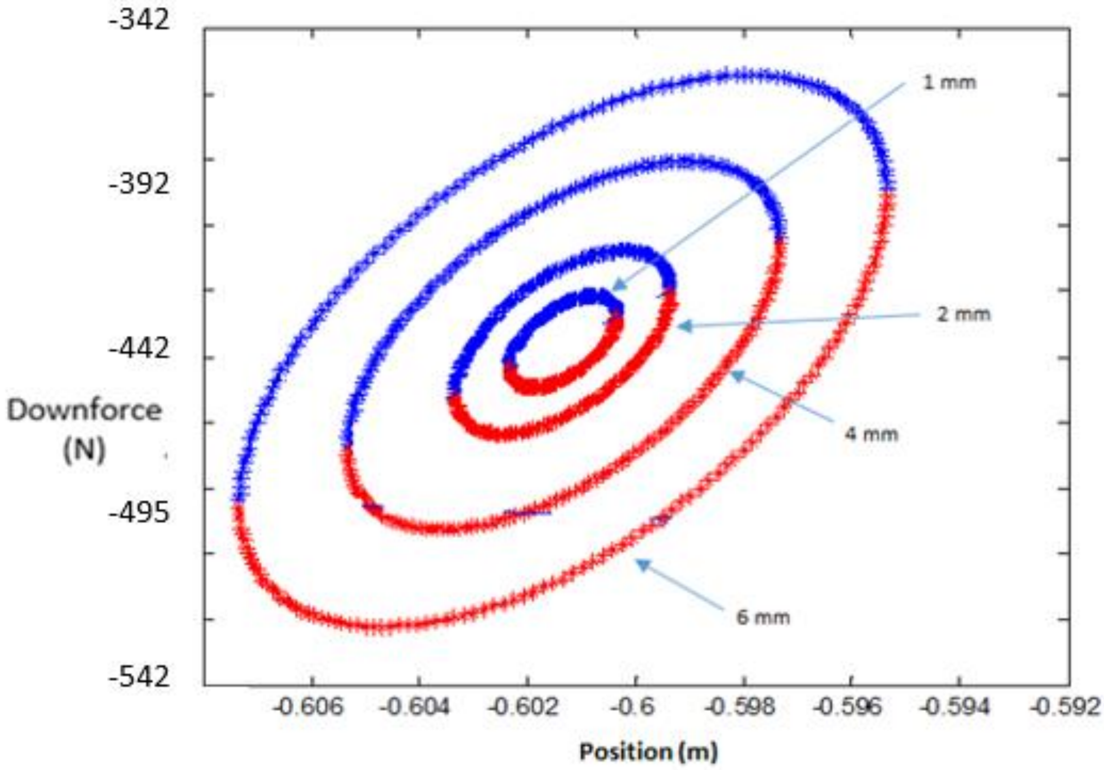

Fig.15: 99Hz: Amplitudes: 1mm, 2mm, 4mm and 6mm.

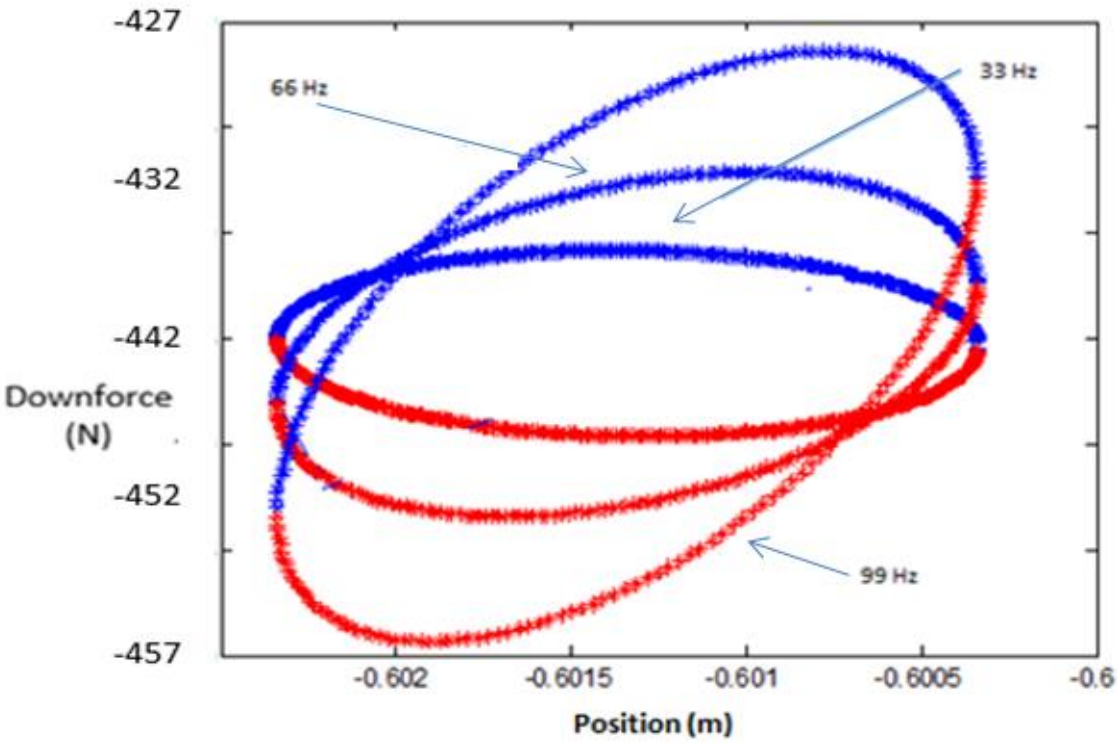

Fig.16: 1 mm Amplitude: 33Hz, 66Hz and 99Hz.

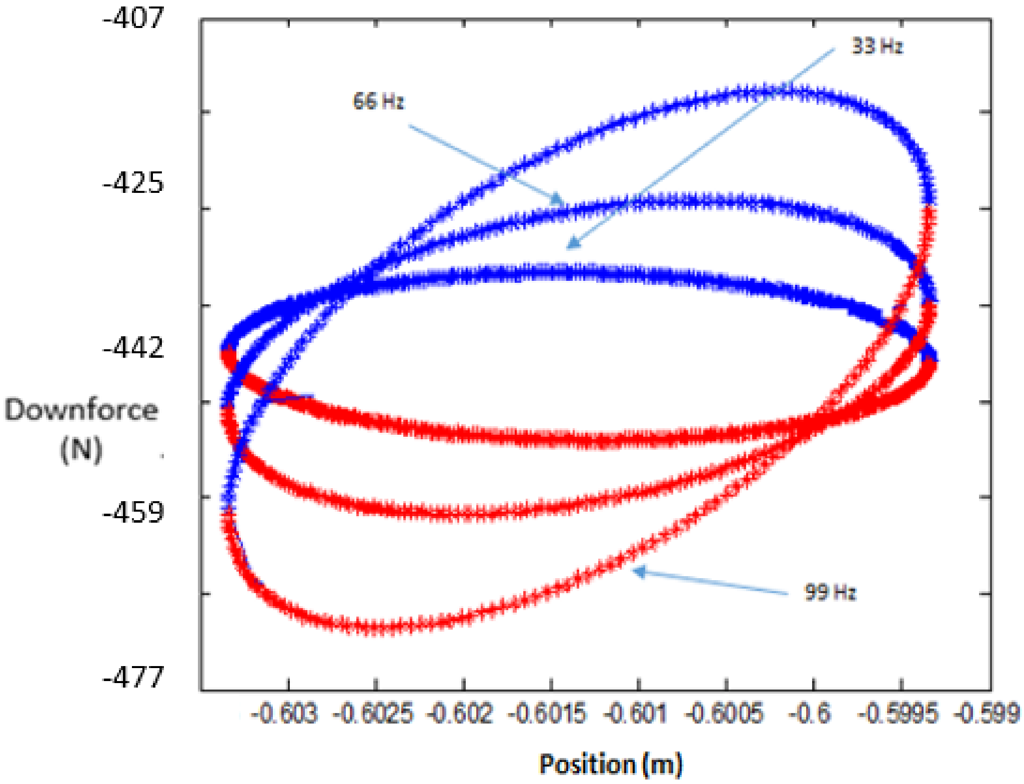

Fig.17: 2mm Amplitude: 33Hz, 66Hz and 99Hz.

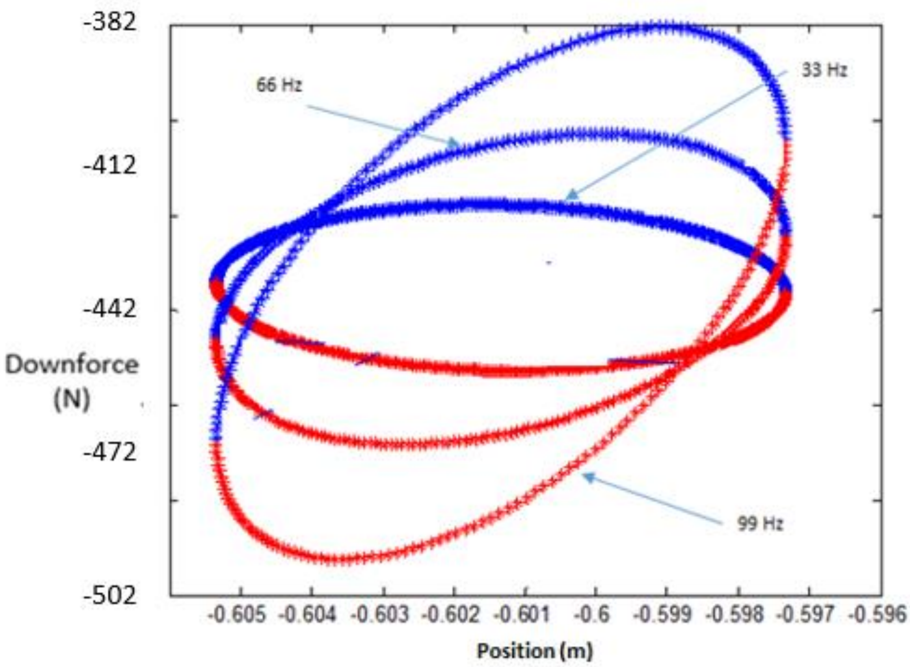

Fig.18: 4mm Amplitude: 33Hz, 66Hz and 99Hz.

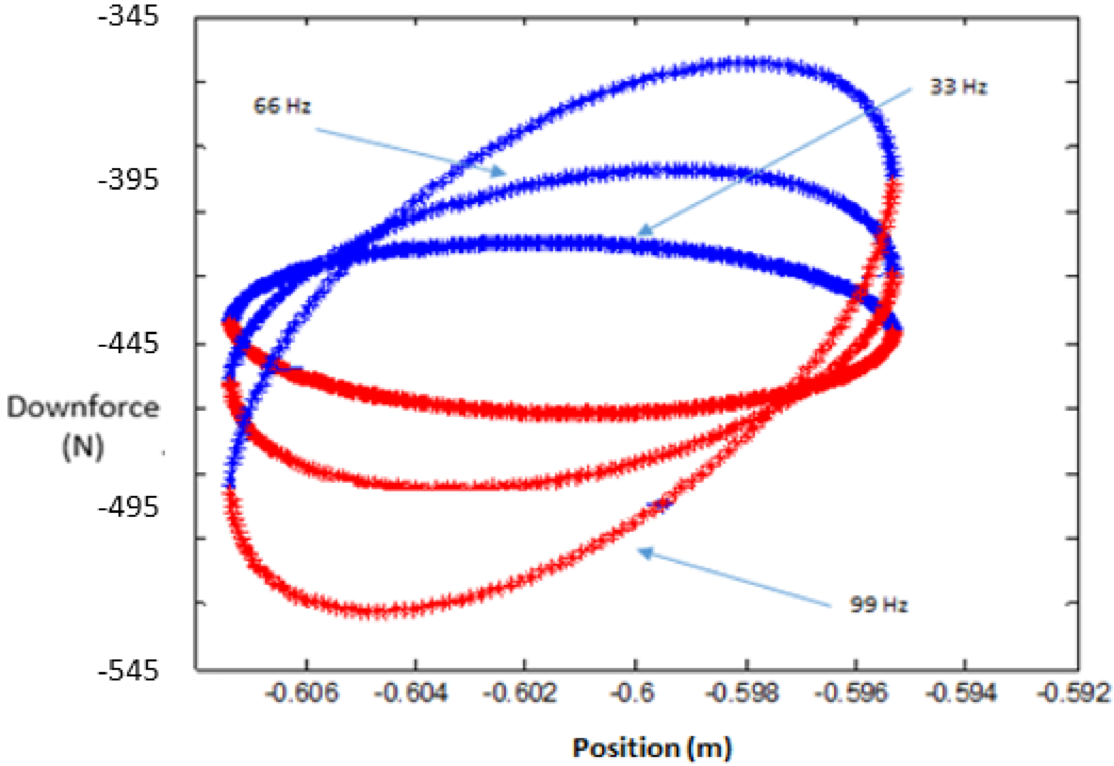

Fig.19: 6mm Amplitude: 33Hz, 66Hz and 99Hz.

Is possible to see that if the frequency or displacement is greater, the downforce also is greater.

For the moment and in every frequency, show it only one period (the first period full) (Fig.20):

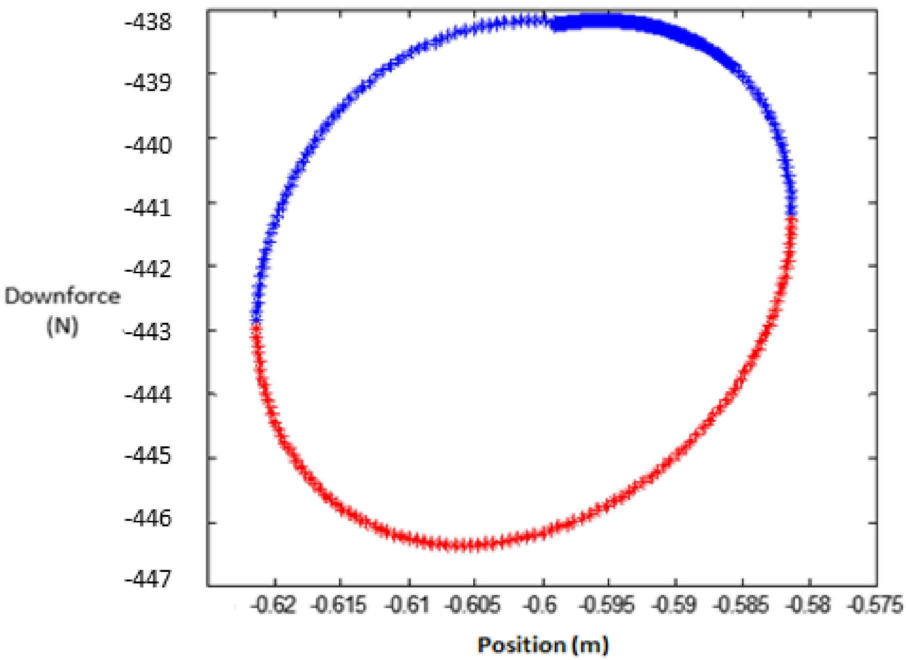

Fig.20: 1Hz full first period.

But if it representing more periods, the geometry generated is different (Fig.21, 22, 23, 25 and 25):

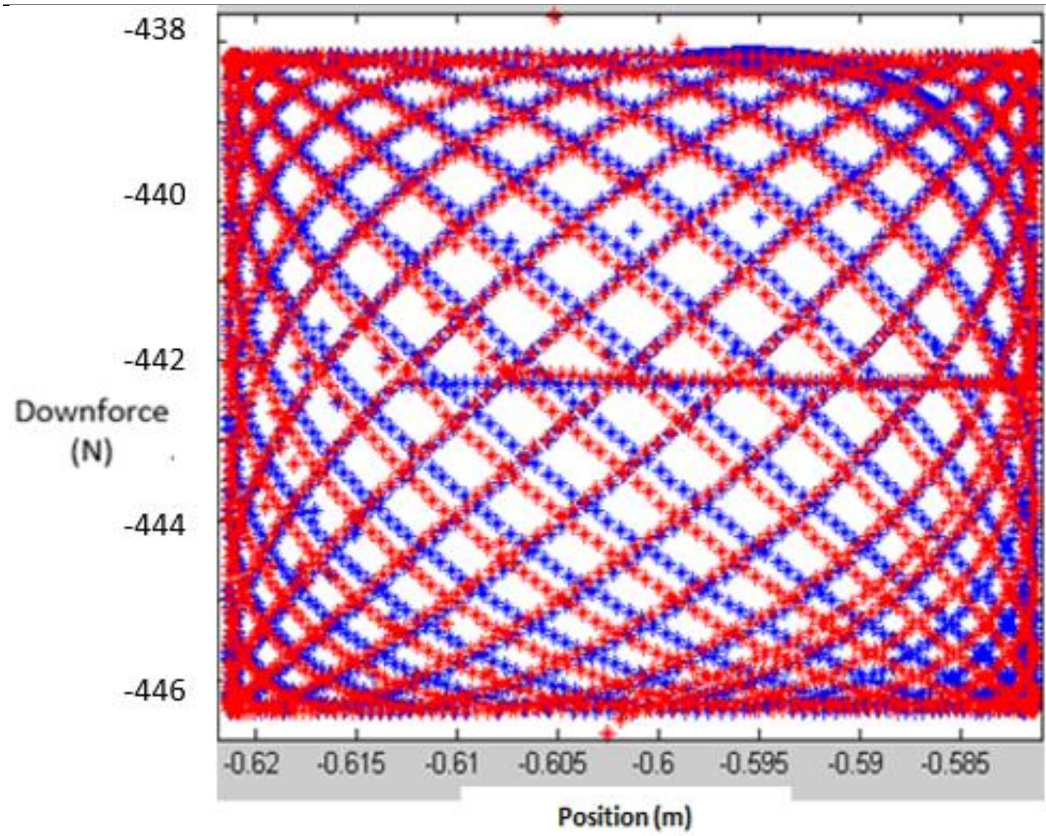

Fig.2

1: 1Hz:

The same representation with another frequencies and periods:

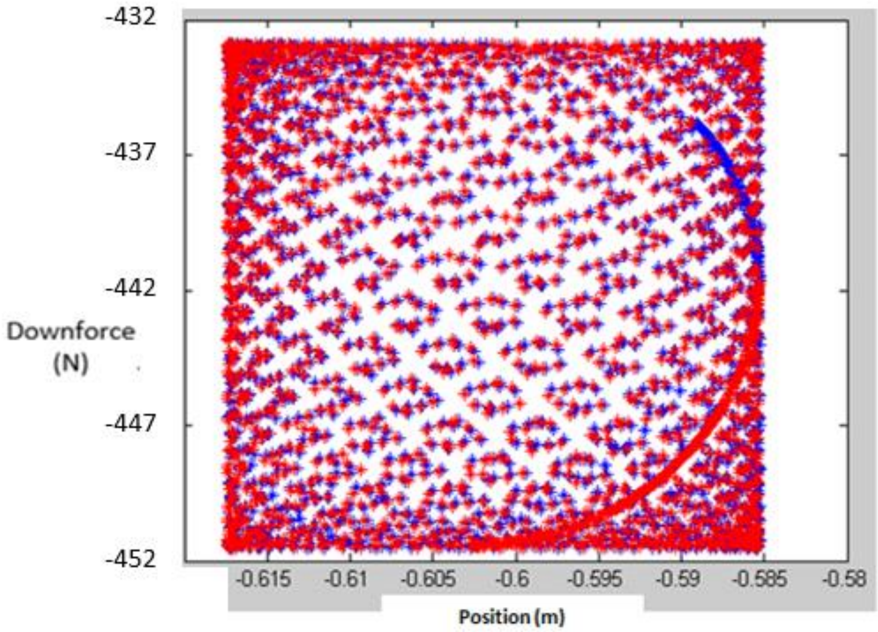

Fig.22: 3Hz:

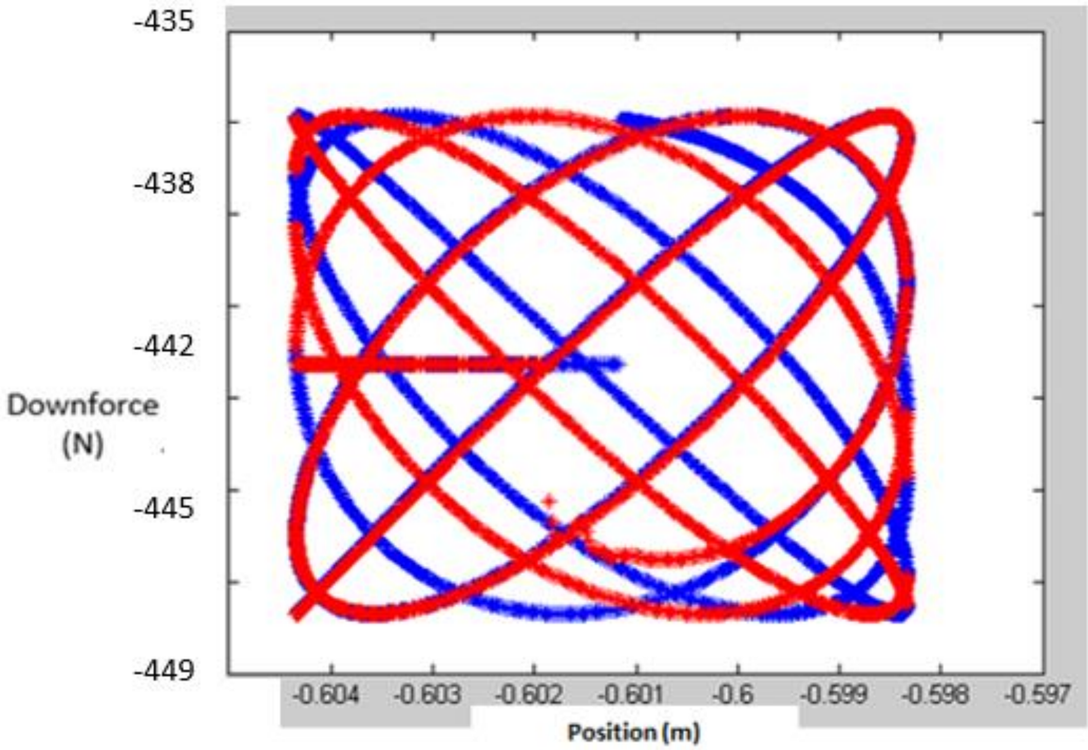

Fig.23: 10Hz:

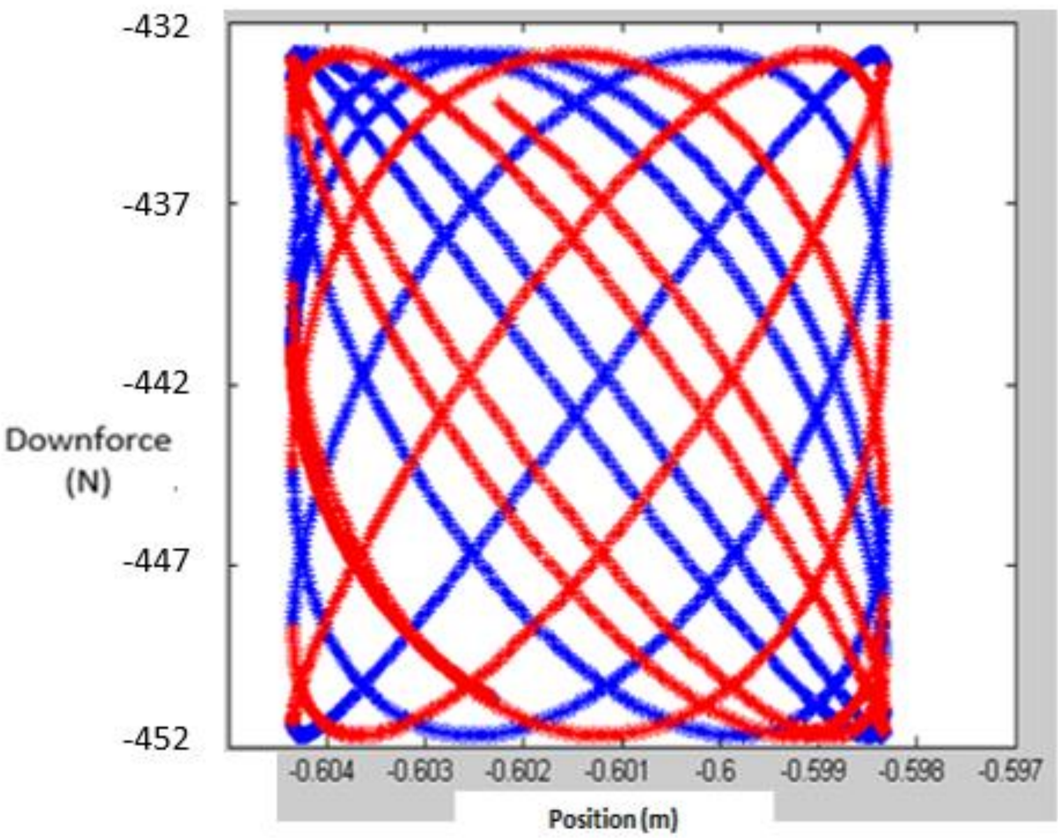

Fig.24: 20HZ

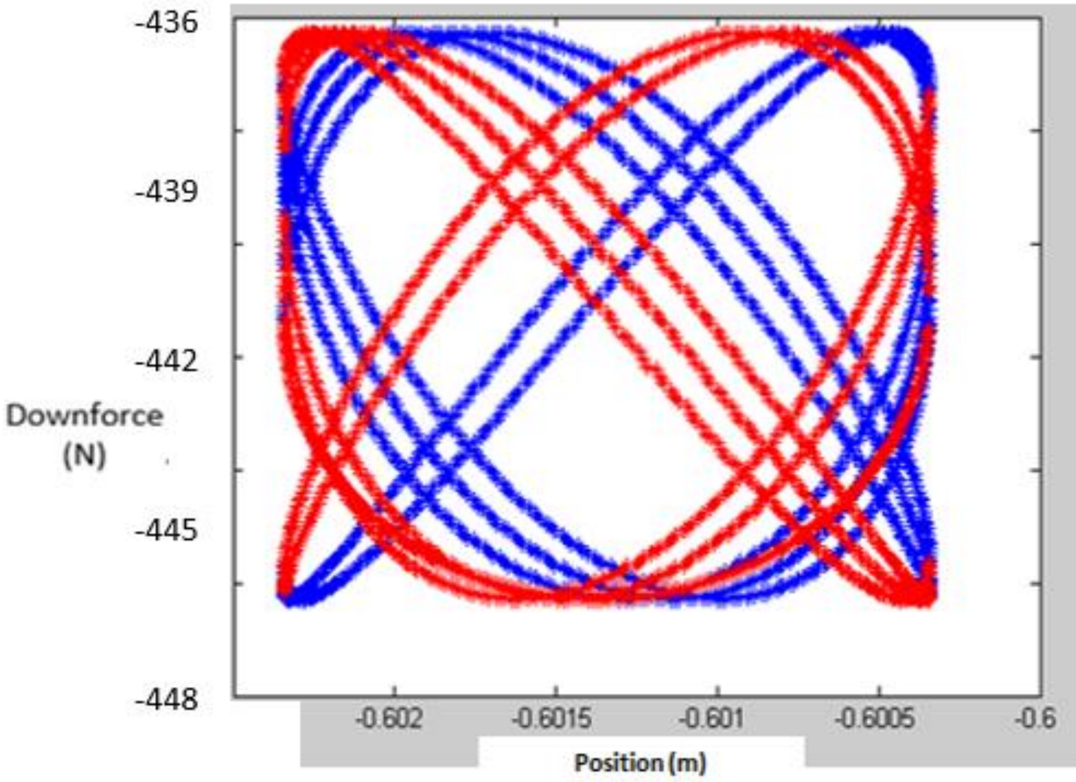

Fig.25: 40HZ

Can now appreciate, many downforce values obtained for the same position in height: the non-linearity is present; that is a problem, because is not possible to create a Function Transfer between all frequencies and downforce.

The most important is that the gain is always the same for one frequency, not the phase:

2. TRANSIENT ANALYSIS

When the vehicle takes an irregularity, it is in the initial moment when it reacts, hence want to use the "first" transient downforce values; for this, the study will be based on Lissajous curve calculated on average between the first two periods.

2.1. TRANSFER FUNCTION GENERATION

It work about the TF system generation between displacement-input (frequencies) and downforce-output (Fig.26); that is the objective:

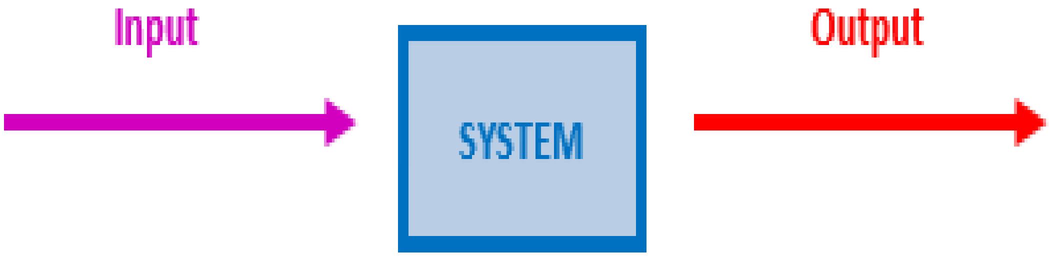

Fig.26: Input and output signal.

For that, is necessary creating the bode plot and from him, generate the TF. About the generation Bode plot, first it show the Gain (in decibels) versus Frequency (Fig.27) and the nomenclature:

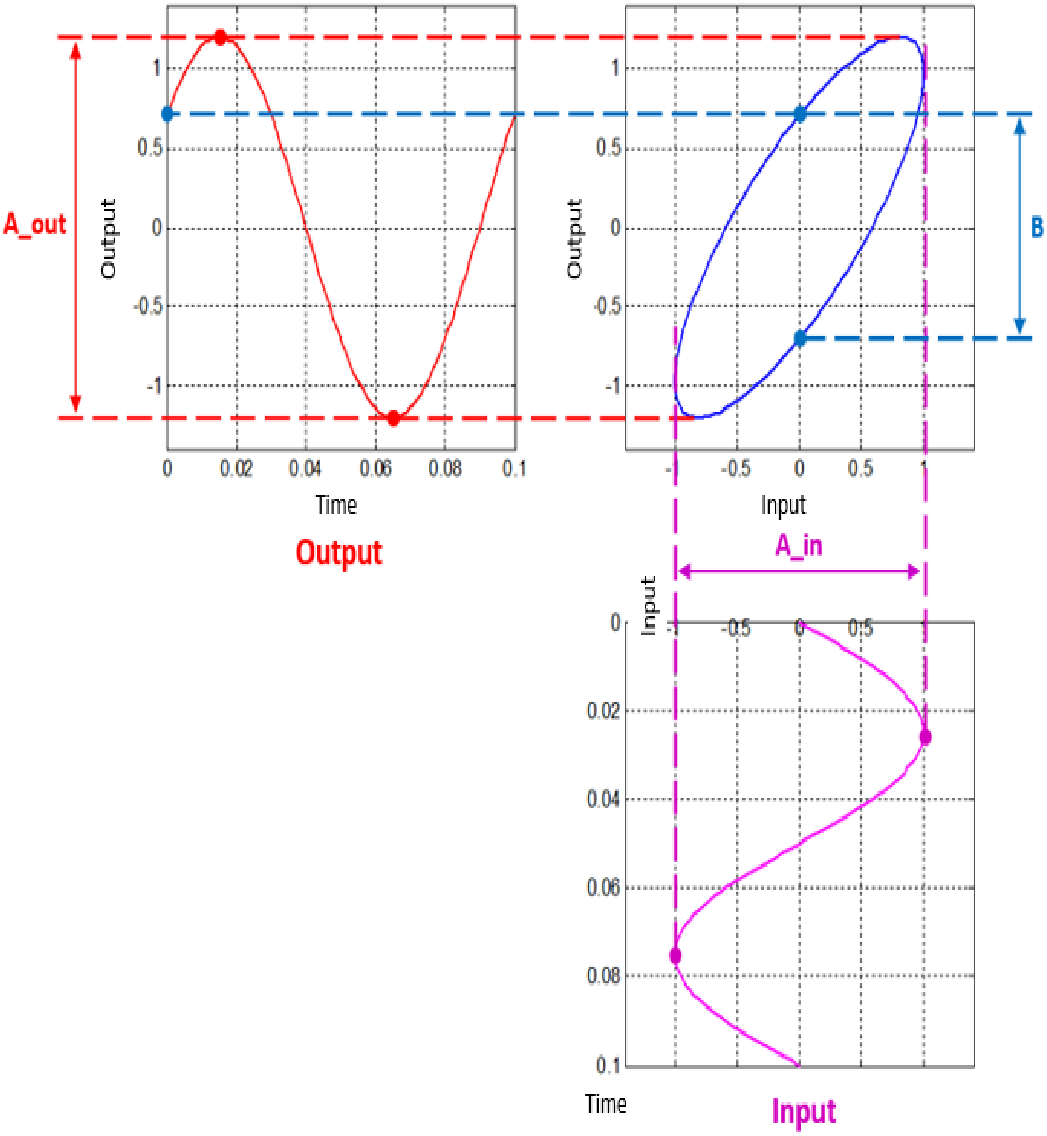

Fig.27: Representation Lissajous curve and geometry values.

The gain in dB is (Eq.2):

$$Am(dB) = 20\log_{10}\left(\frac{O}{I}\right)$$ Eq.2: Gain in dB.

Show it the gain for every frequency (Table 1 and Fig.28):

Hz	A_out (N)	A_in (mm)	Gain
1	8,20	20,00	-7,74
5	22,80	12,00	5,58
10	10,80	3,00	11,13
25	14,70	2,00	17,33
33	17,40	2,00	18,79
38	9,60	1,00	19,65
66	16,20	1,00	24,19
500	94,00	0,20	53,44
800	128,30	0,10	62,16

Table 1: Gain against frequencies.

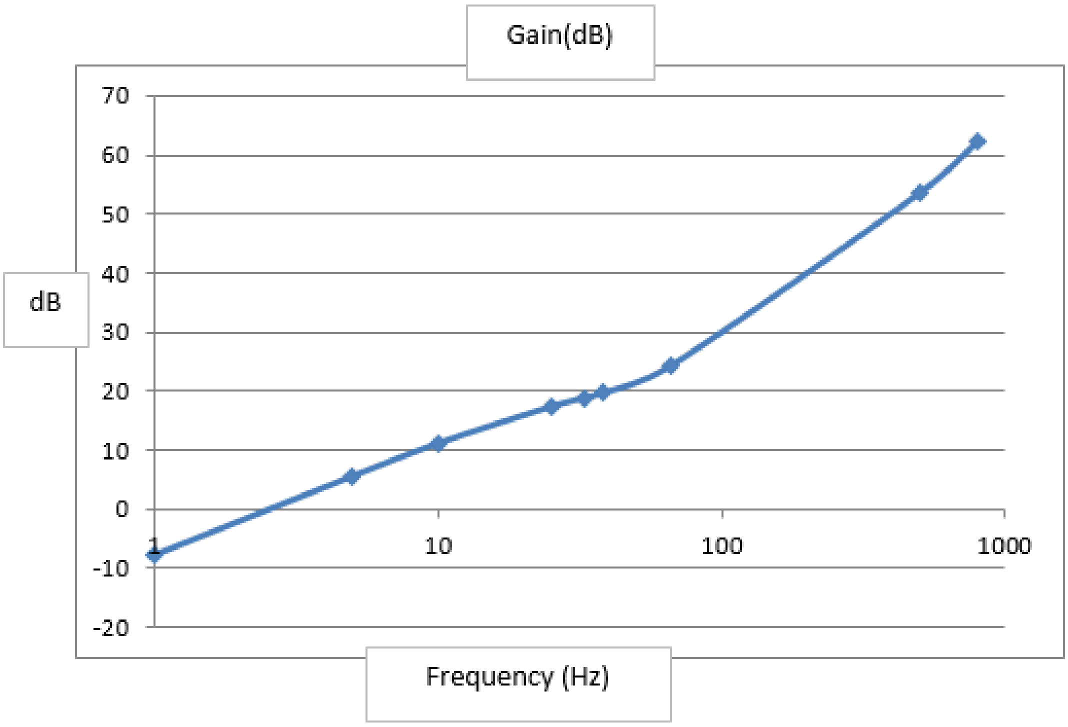

Fig.28: Gain against frequencies.

About the delay or phase between input “I” and output “O” (Fig.29):

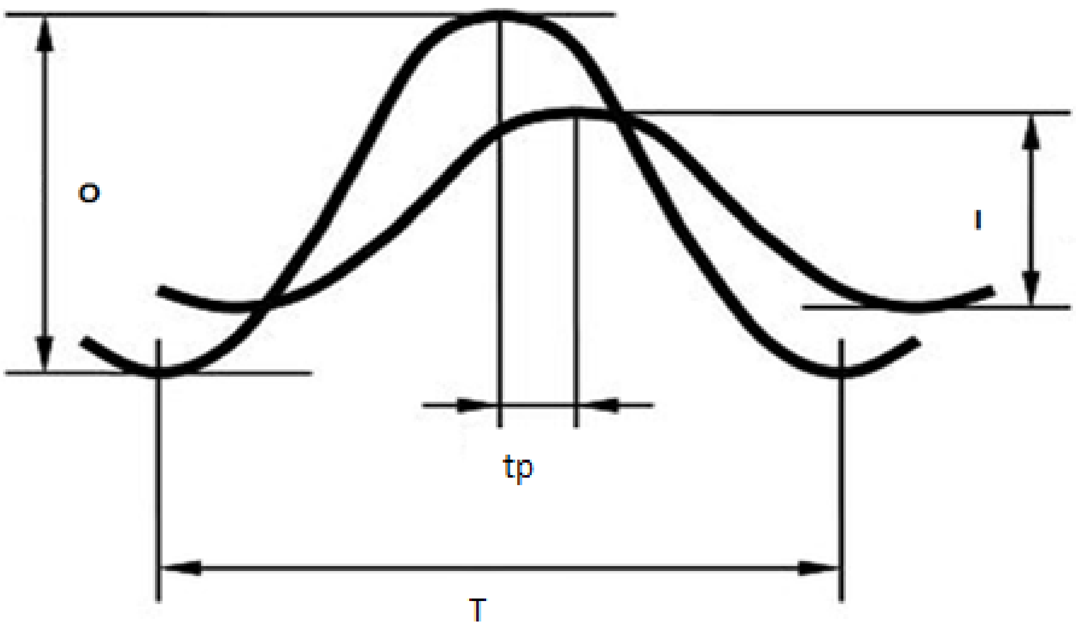

Fig.29: Input and output delay.

The phase in degrees is (Eq.3):

$$\theta(^{o}) = \frac{360tp}{T}$$ Eq.3: Phase in degrees.

Show it the delay or phase for every frequency (Table 2 and Fig.30)):

Hz	Phase (º)
1	63,00
5	90,00
10	94,58
25	95,16
33	92,67
38	92,06
66	71,52
500	18,00
800	27,00

Table 2: Phase against frequencies.

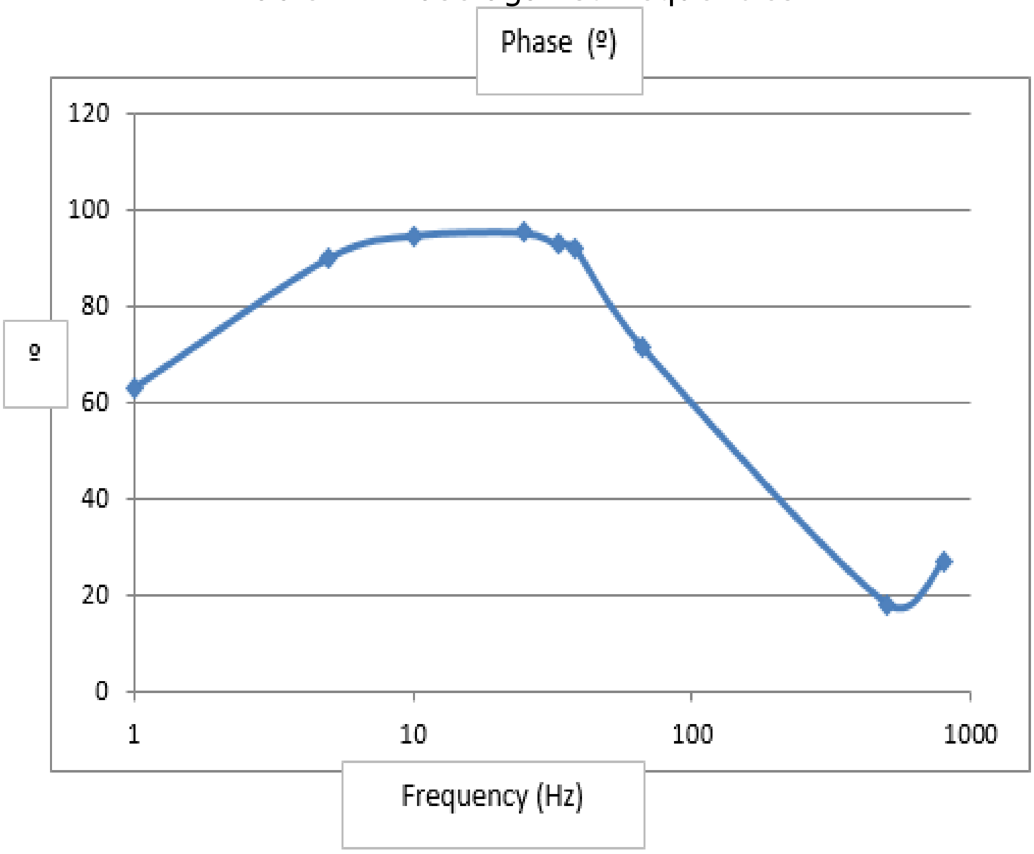

Fig.30: Phase against frequencies.

From this bode plot, is possible to calculate the TF.

It work with a Matlab tool (System Identification) in order to calculate the Transfer Function (Estimated) from a values CFD.

It suppose that exist 4 Zeros and 4 Poles (Eq.4); so:

Fit to estimation data (Matlab tool): 99.96% (filter focus); FPE: 0.06247, MSE: 0.03224

$$\frac{-2445000\,s^{4}-1147\,10^{7}\,s^{3}+1108\,10^{10}\,s^{2}-2274\,10^{12}\,s-6536\,10^{12}}{s^{4}-2089\,s^{3}+5.418\,10^{7}\,s^{2}+2.766\,10^{11}\,s-3.681\,10^{13}}$$

Eq.4: Transfer Function estimated, with 4 zeros and 4 poles.

The bode plot of Eq.4 is (Fig.31):

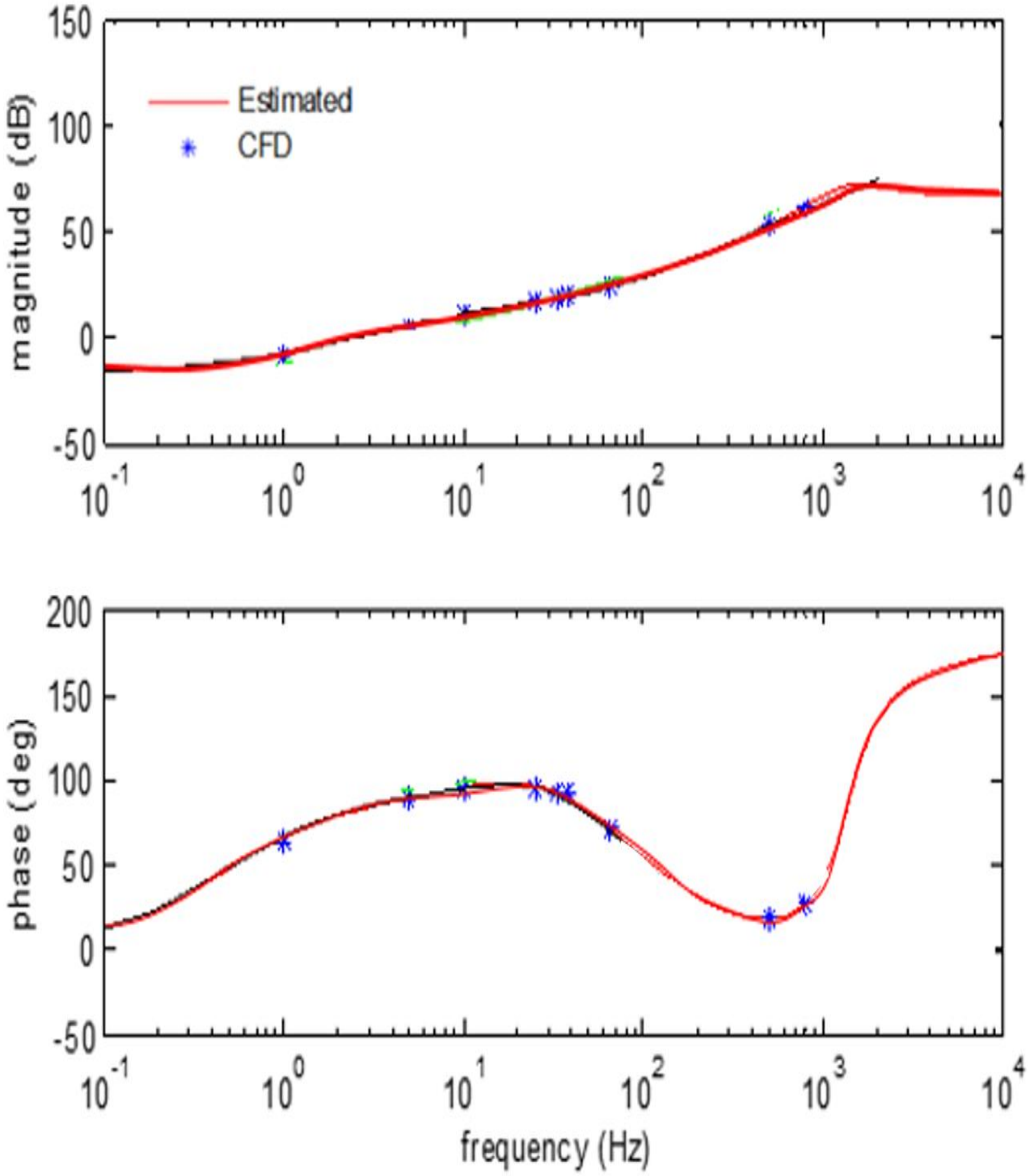

Fig.31: Bode Plot Transfer Function (Eq.4) against points values from CFD.

Working it with this Transfer Function, there is a problem: the dynamic system evolution with this TF is not stable (Theorem Routh-Hurwitz); that is because the poles and zeros are in semiplane right (Fig.32):

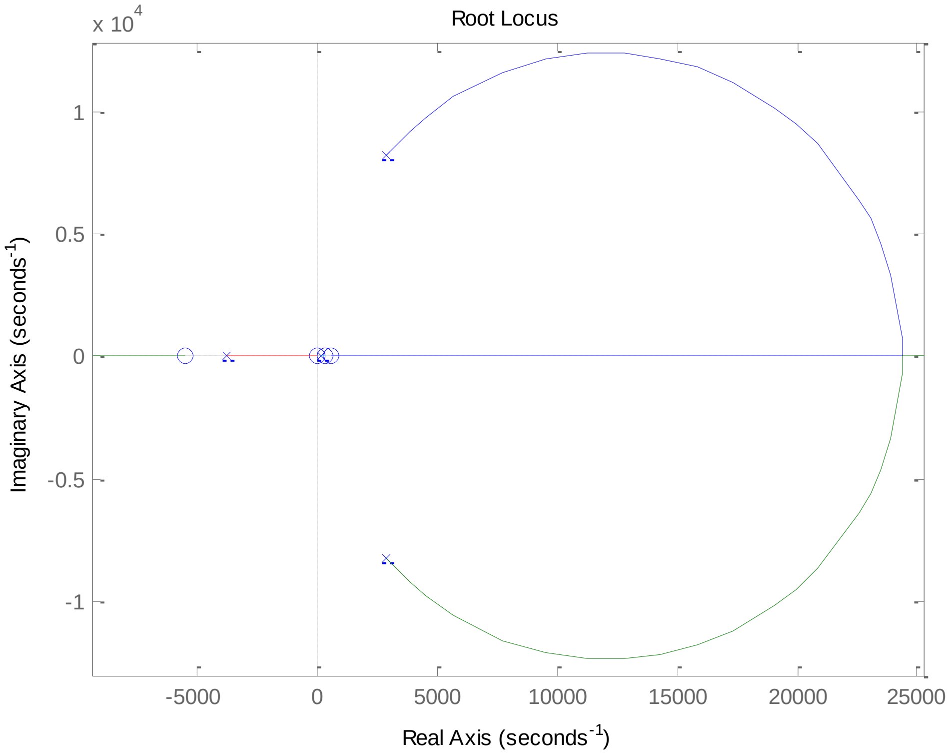

Fig.32: Localization poles and zeros TF:

In order to convert the TF in stable is necessary to translate poles and zeros to semi plane negative (Fig.33); that process creates a new Transfer Function (Eq.5); this process is made with Matlab command directly:

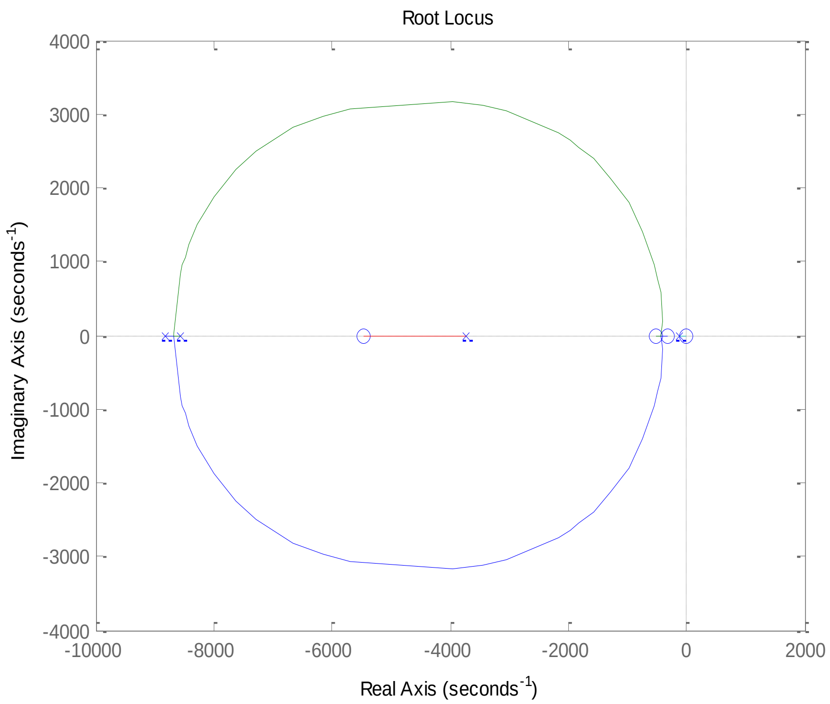

Fig.33: New localization poles and zeros TF.

$$\frac{2461000\,S^{4}+1558\,10^{7}\,S^{3}+1192\,10^{10}\,S^{2}+2319\,10^{12}\,S+6151\,10^{12}}{S^{4}+2.125\,10^{4}\,S^{3}+1.432\,10^{8}\,S^{2}+3.002\,10^{11}\,S+3.645\,10^{13}}$$

Eq.5: New stable TF.

Now, the new Bode plot is (Fig.34); that Transfer Function is stable:

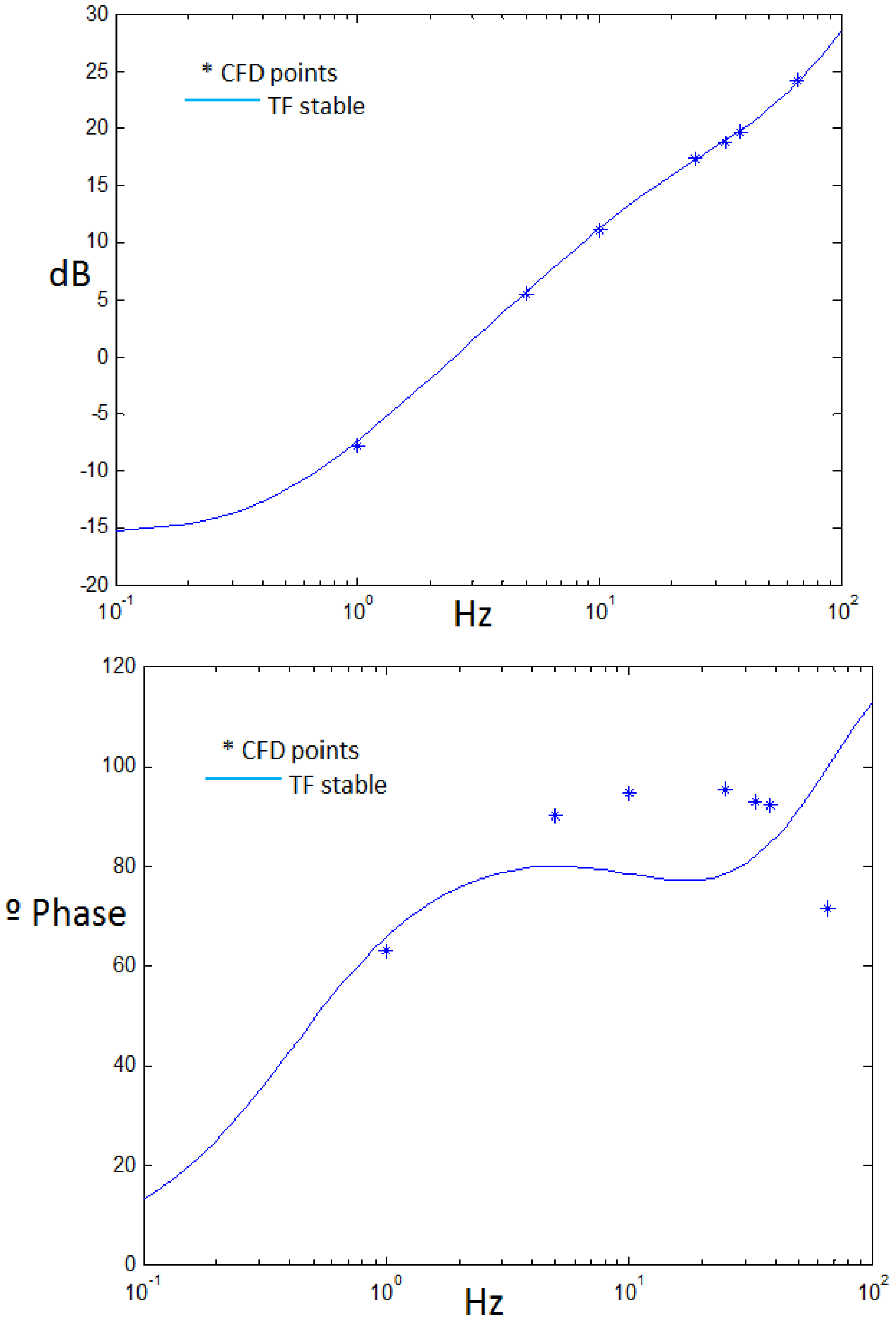

Fig.34: Bode Plot TF stable, with CFD points comparison.

There is a little difference in phase (not important), not in gain. That will be the TF for this article.

3. APPLICATION: ¼ MODEL CAR

The principal goal now, is applied this procedure (TF aerodynamic) into a car; for that and in the first step, is applied to quarter car model. As we was say before, from this procedure it will be possible to know the car behavior really; that is: with the aerodynamics values transients.

3.1. TEST VALUES, CONDITIONS AND RESULTS WITHOUT AERODYNAMIC

In this model the tire is represented with a spring (k_u) and damper (C_u); the suspension system as a spring (k_s) and a damper (c_s); sprung mass in the car is represented by "m_s" and unsprung mass by "m_u" (Fig.35):

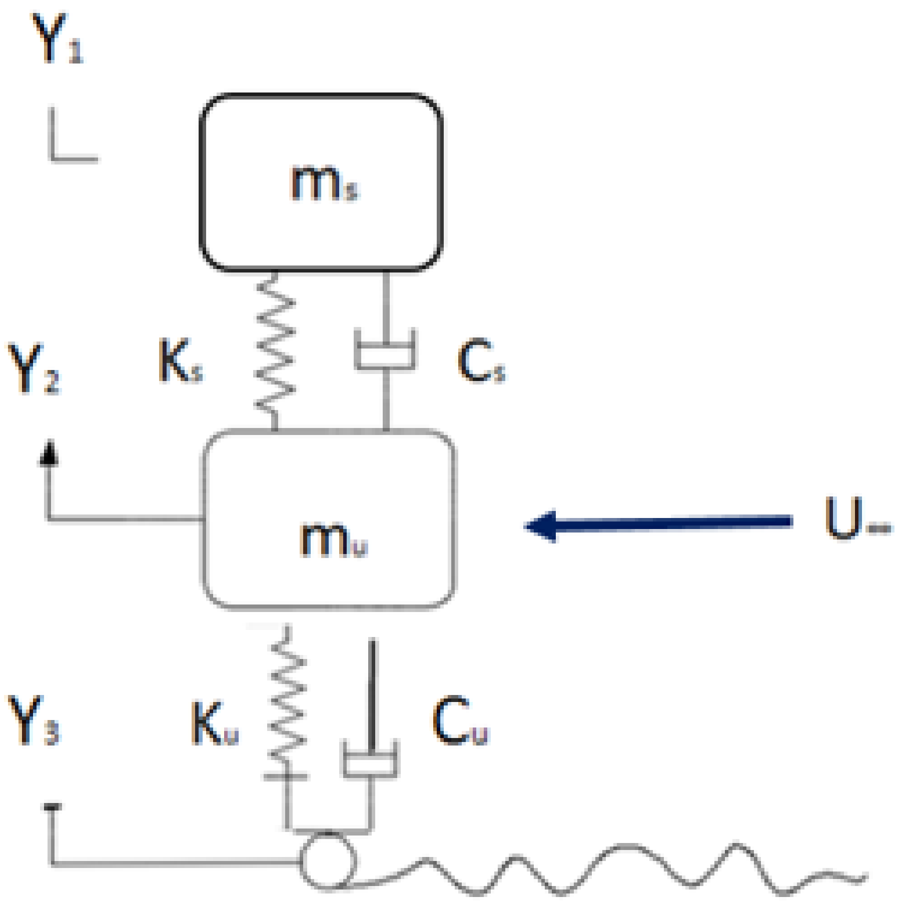

Fig.35: Quarter car model.

Data values (Table 3):

Sprung Mass	35 Kg
Unsprung Mass	5 Kg
Spring Suspension	40000 N/m
Damper Suspension:	1600 N/ms
Spring Tyre	46000 N/m
Damper Tyre	0,2 N/ms

Table 3: Values test.

The tests consists in:

It applied one vertical ("y" direction) impulse as input (to unsprung mass); the input (as a track) value is a signal of 400 N while 2 milliseconds.

It works with a typical quarter model; the equations are (Eq.6):

$$m_s\ddot{y}_1 + c_s(\dot{y}_1 - \dot{y}_2) + k_s(y_1 - y_2) = 0$$
$$m_u\ddot{y}_2 + c_s(\dot{y}_2 - \dot{y}_1) + c_u(\dot{y}_2 - \dot{y}_s) + k_s(y_2 - y_1) + k_u(y_2 - y_1) = k_u y_3$$

Eq.6: Quarter car model without aerodynamics.

The goal is know the TF influence into quarter car model; so is necessary to know the dynamic behavior quarter model without transients aerodynamic; the values are (Fig.36 and 37):

Sprung mass vertical motion (Fig.36):

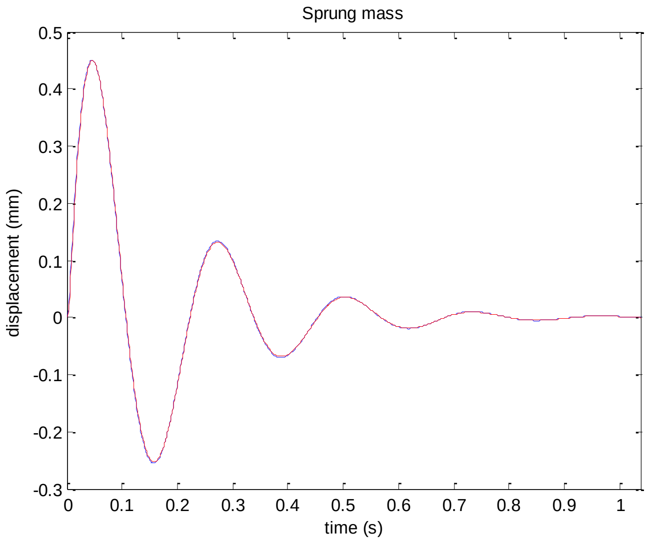

Fig.36: Sprung mass vertical motion

Unsprung mass vertical motion (Fig.37):

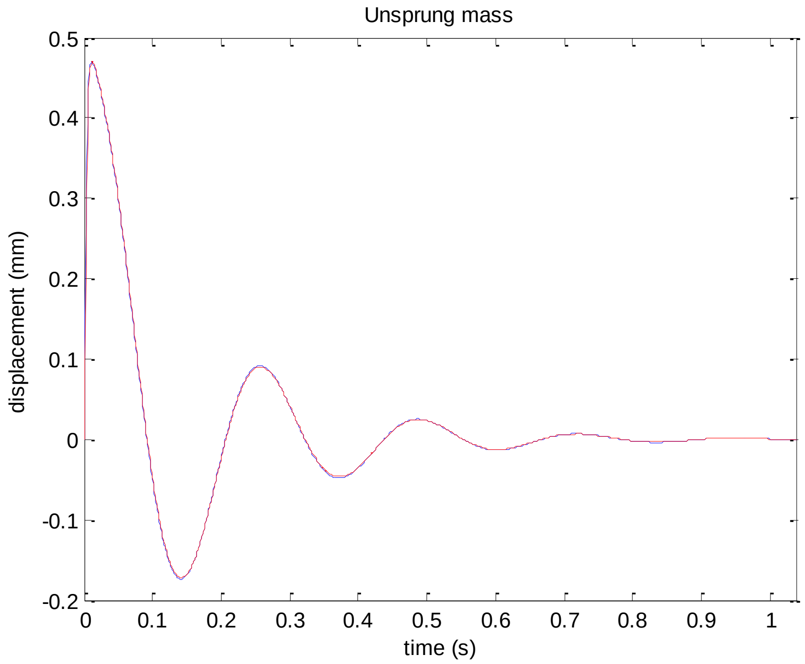

Fig.37: Unsprung mass vertical motion

This evolution will be the base for the comparison.

3.2. TEST VALUES AND MODEL WITH TRANSFER FUNCTION AERODYNAMIC

Now, the quarter car model used, with aerodynamic transients forces is (Fig.38):

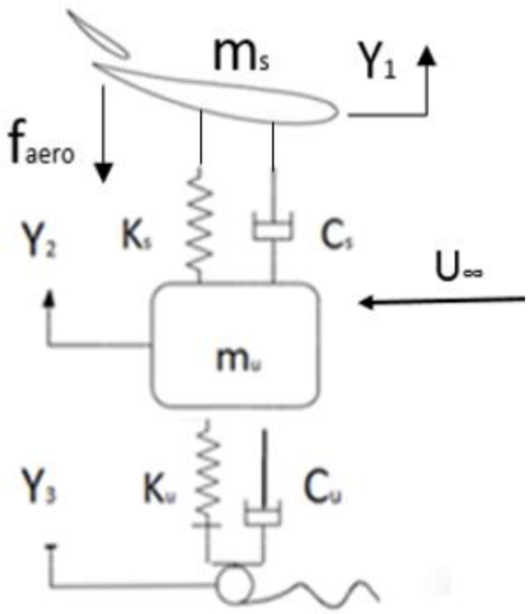

Fig.38: Quarter car model with aerodynamic transfer function.

The values are the same as point 3.1.

The equations are (Eq.7), with "f_{aero}" as a transfer function:

$$m_s\ddot{y}_1 + c_s(\dot{y}_1 - \dot{y}_2) + k_s(y_1 - y_2) = -f_{aero}$$
$$m_u\ddot{y}_2 + c_s(\dot{y}_2 - \dot{y}_1) + c_u(\dot{y}_2 - \dot{y}_s) + k_s(y_2 - y_1) + k_u(y_2 - y_1) = k_u y_3$$

Eq.7: Equations quarter car model with aerodynamic transfer function.

4. REAL TEST DESCRIPTION: RESULTS VALIDATION

The goal is validate the results with TF, against real test; but is very complicate to have a "real" test in this case; in virtual wind tunnel (CFD) that is possible; it considered this simulation, are the results more realistic.

4.1. CFD "REAL" TEST VALUES

In order to avoid the "real" Virtual Wind Tunnel test, the following simulations are performed:

- Geometry (wings combination) as a sprung mass in model Fig.38; the geometry to test is: (two profiles Naca 4612) ; is the same geometry as point 1.1, but 400 mm of span (Fig.39) and 21.117º of angle incidence (Fig.40).
- Spring and damper, as a tire (among mass as unsprung mass).
- Spring and damper as suspension (between sprung and unsprung mass).
- Signal input by impulse (400 N while 2 milliseconds).
-

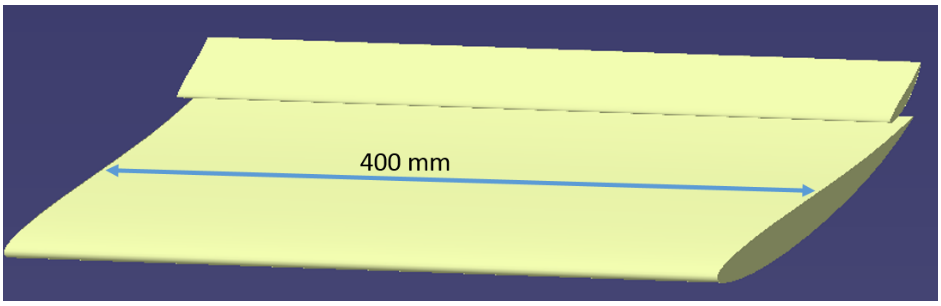

Fig.39: Span geometry.

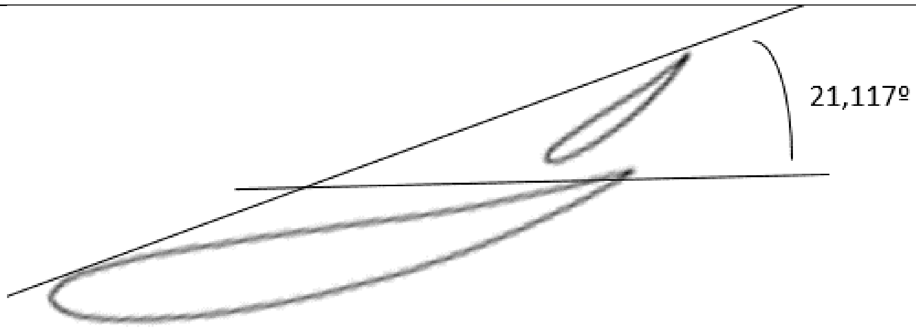

Fig.40. Incidence angle.

The tests consist in: it is the quarter model car on the road; is applied as examples, a stream of air at 30, 50 and 69.4 m/s and is observed that the suspension and tires deflect to an equilibrium position in time; it is that time is applied an impulse as input; the input value is a signal of 400 N in 2 milliseconds, when the initial downforce is stabilized.

In these tests, there are two periods or zones so:

a. Stabilization in position and downforce (Fig.41).
b. Input signal and system dynamic evolution (Fig.42).

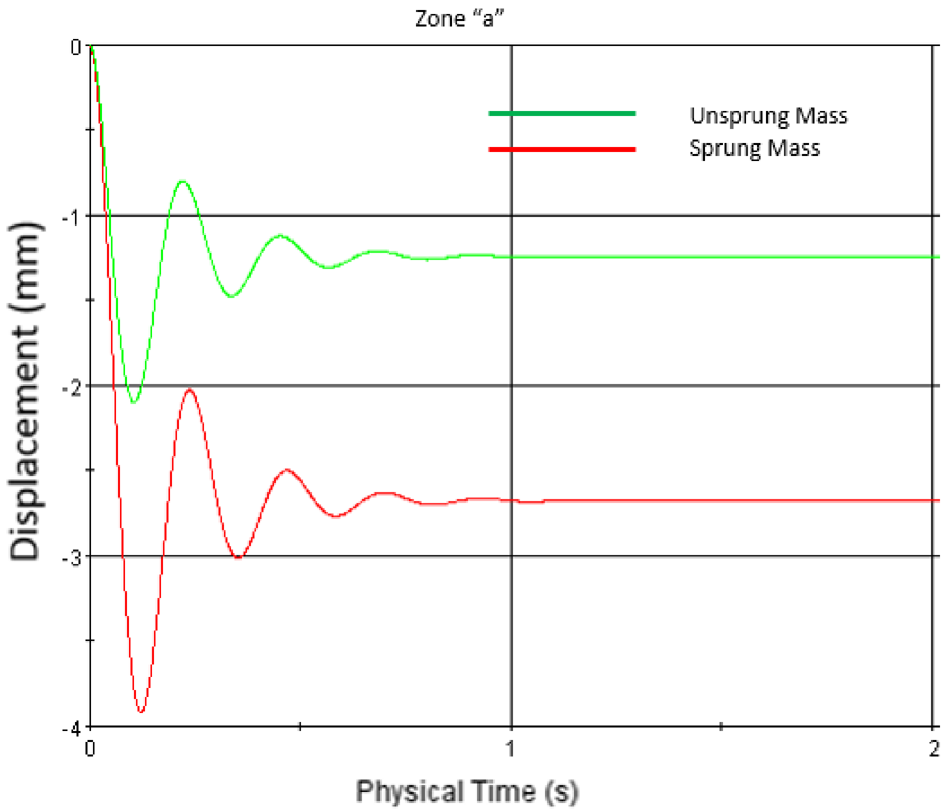

Fig.41: Stabilization period – 30 m/s

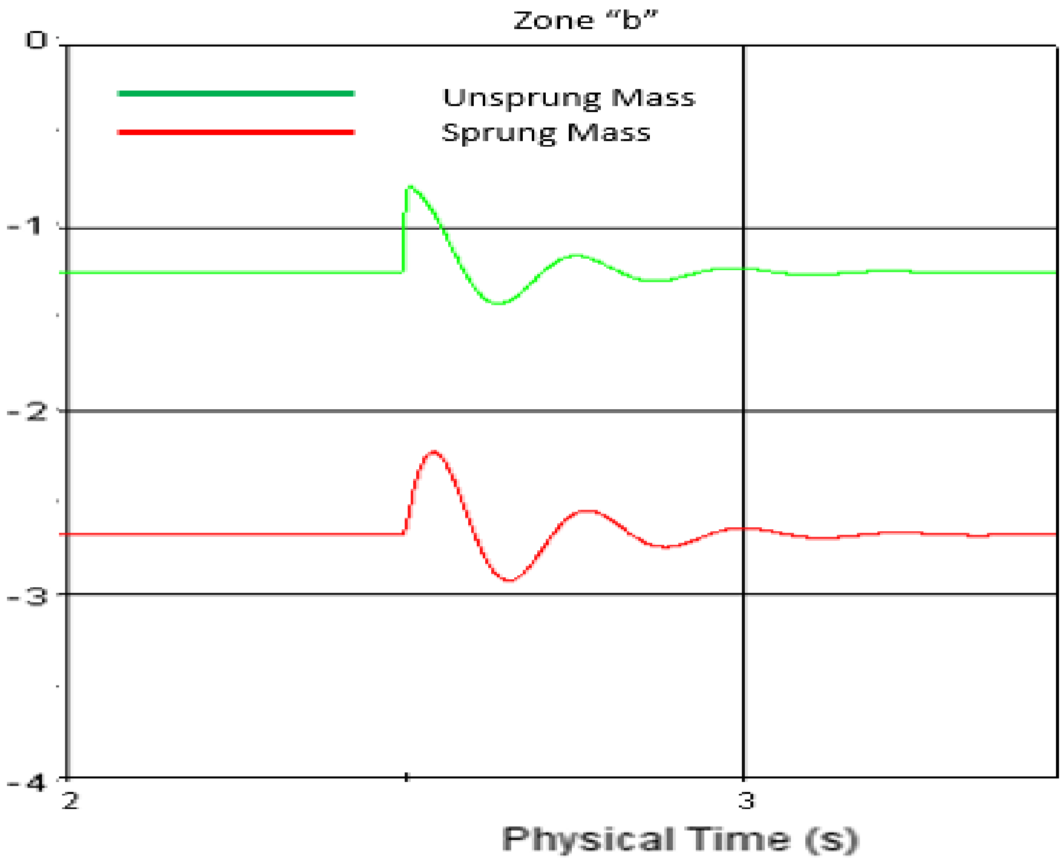

Fig.42: Impulse period – 30 m/s

4.1. GRAPHICAL COMPARISON

The objective is to know the speed influence in the dynamic evolution.

4.1.1. QUARTER CAR MODEL WITHOUT AERODYNAMICS FORCES AGAINST QUARTER CAR MODEL IN VIRTUAL WIND TUNNEL – LOW SPEED (30 m/s) WITH IMPULSE 400 N WHILE 2 MILLISECONDS

Show it the displacement of Sprung and Unsprung mass against Time (Fig.43 and 44):

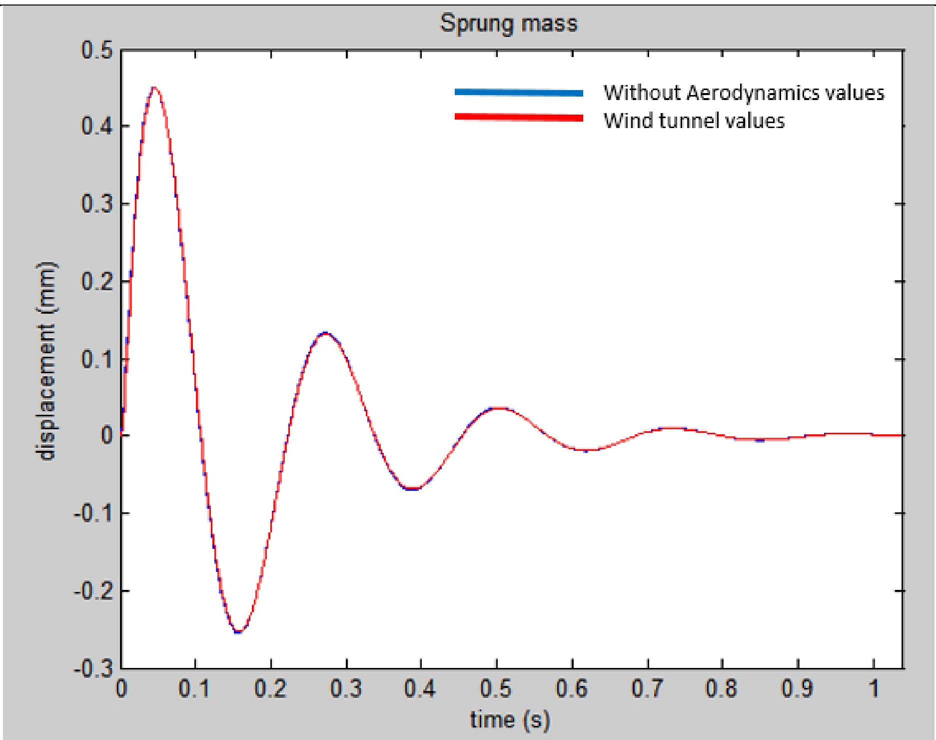

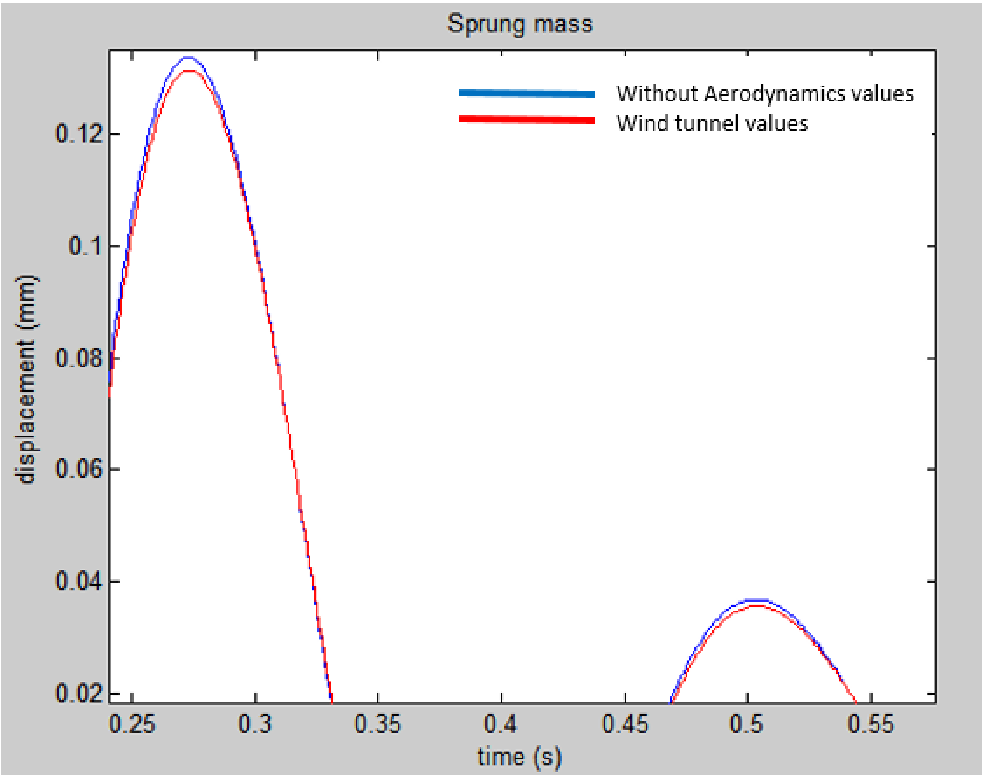

Fig.43: Displacement Sprung mass.
Detail of Fig.43

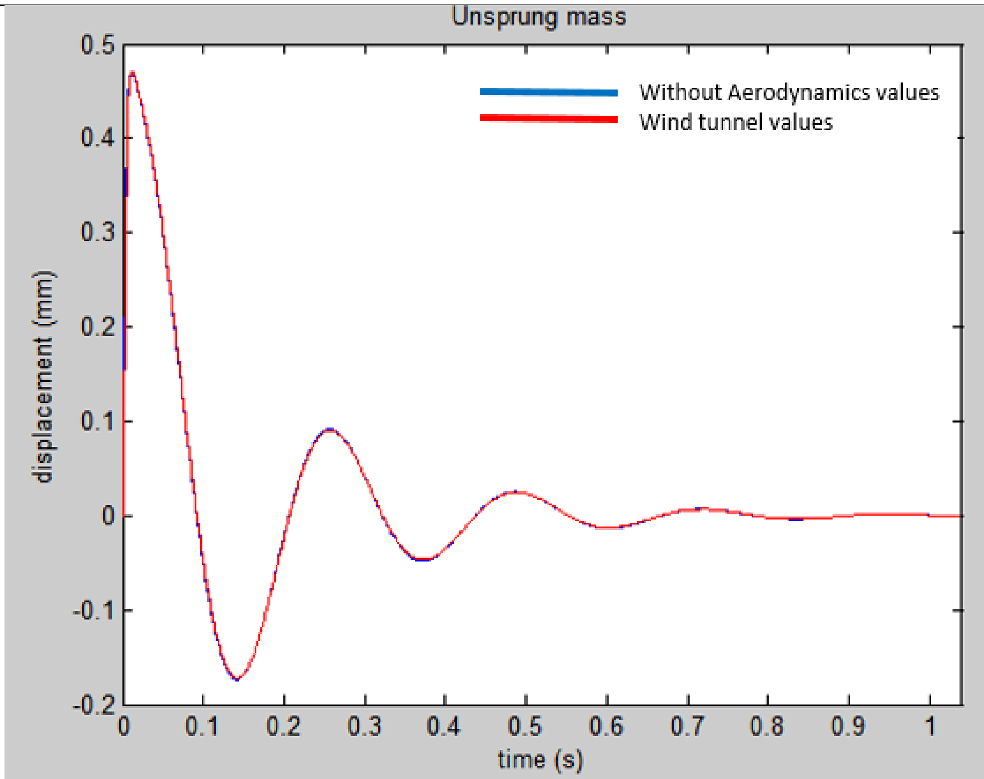

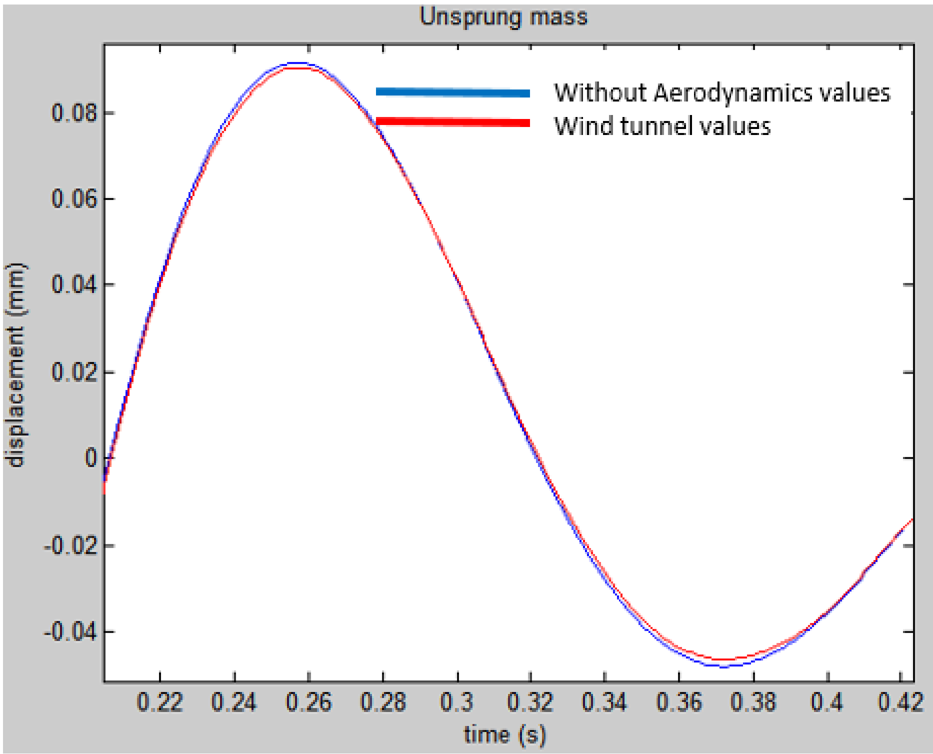

Fig.44: Displacement Unsprung mass
Detail of Fig.44

For low speed, the differences between wind tunnel virtual values and quarter car model, is little.

4.1.2. QUARTER CAR MODEL WITHOUT AERODYNAMICS FORCES AGAINST QUARTER CAR MODEL IN VIRTUAL WIND TUNNEL – MEDIUM SPEED (50 m/s) WITH IMPULSE 400 N WHILE 2 MILLISECONDS

Show it the displacement of Sprung and Unsprung mass against Time (Fig.45 and 46):

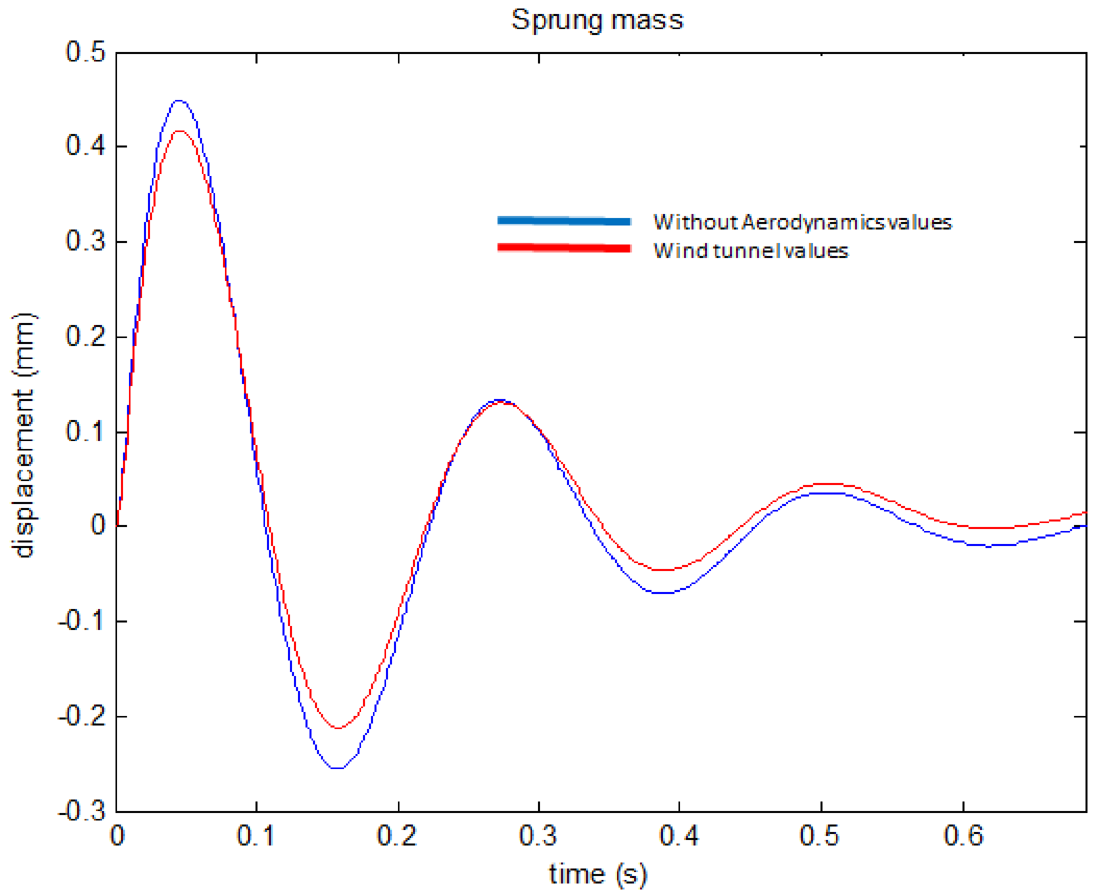

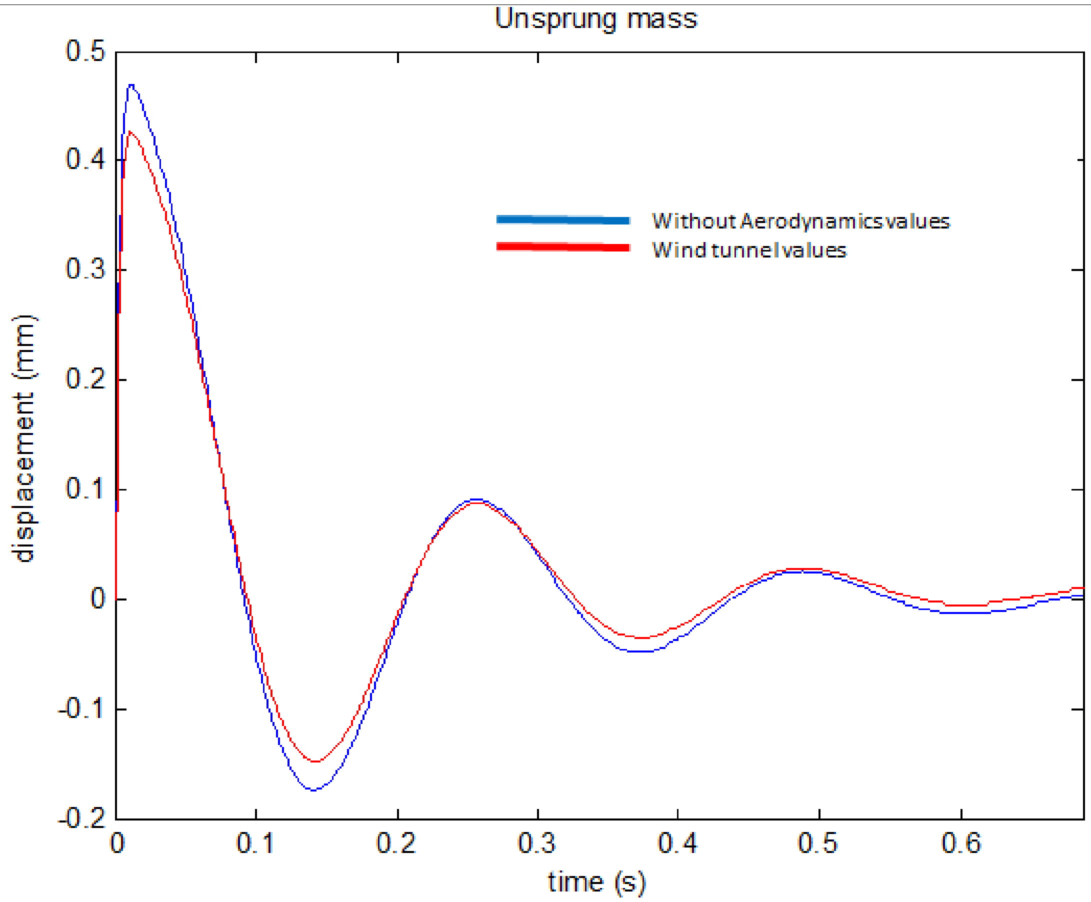

Fig.45: Displacement Sprung mass. Fig.46: Displacement Unsprung mass.

In this case, the differences are greater.

4.1.3. QUARTER CAR MODEL WITHOUT AERODYNAMICS FORCES AGAINST QUARTER CAR MODEL IN VIRTUAL WIND TUNNEL – HIGH SPEED (69.4 m/s) WITH IMPULSE 400 N WHILE 2 MILLISECONDS

Show it the displacement of Sprung and Unsprung mass against Time (Fig.47 and 48):

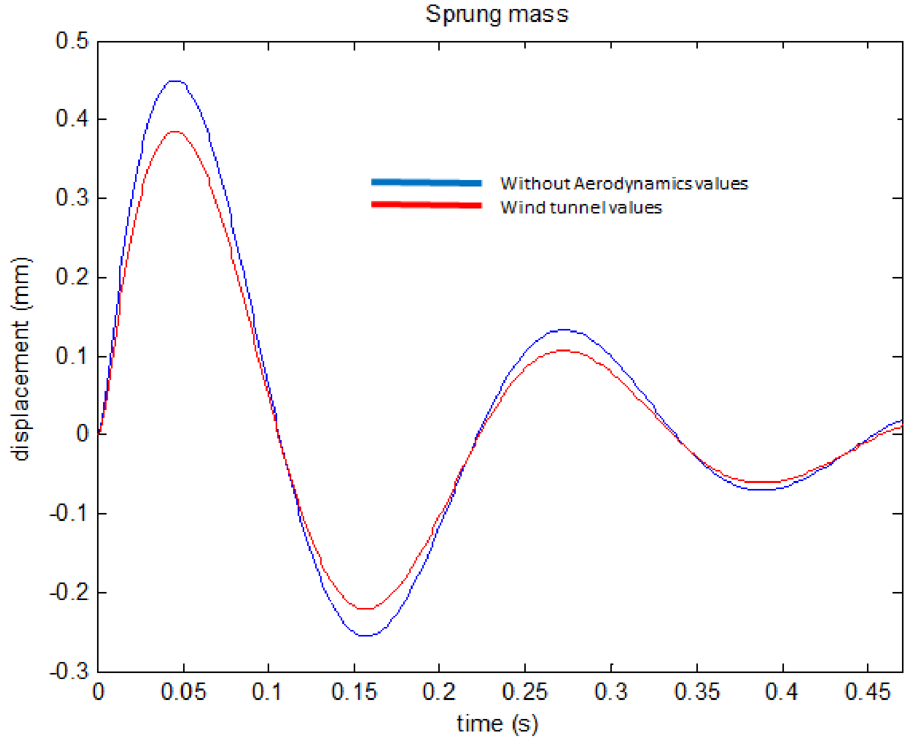

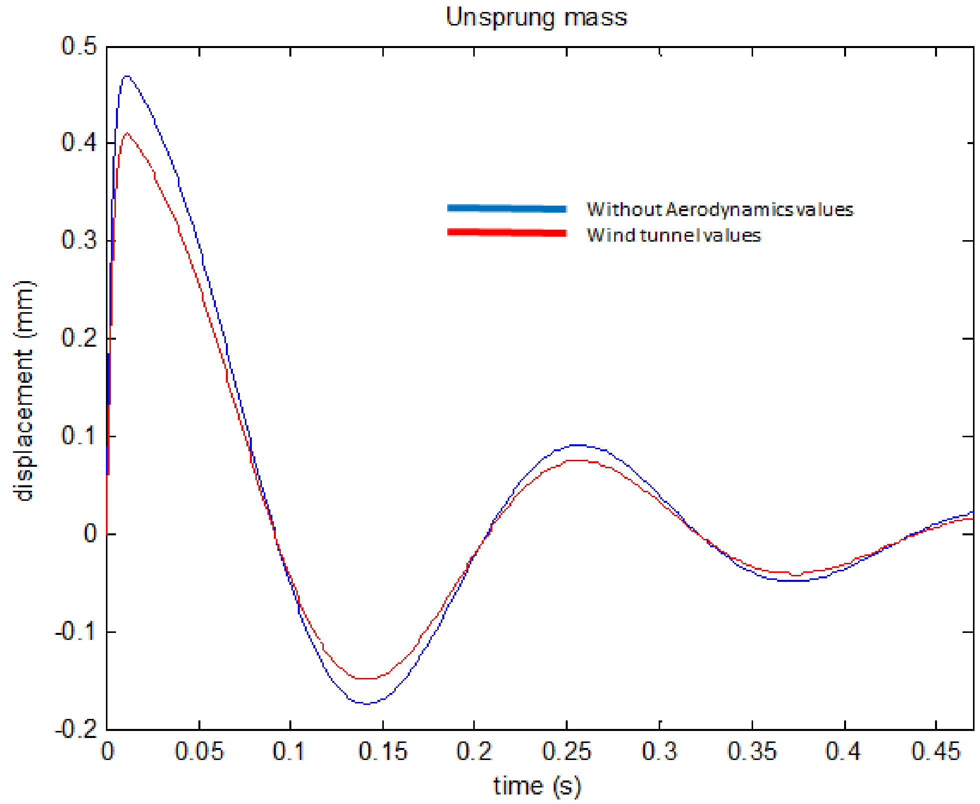

Fig.47: Displacement Unsprung mass. Fig.48: Displacement Unsprung mass.

Finally, the differences between wind tunnel virtual values and quarter car model are big; that is normal: the aerodynamic is a big damper.

5. VALIDATION MODEL ARTICLE: QUARTER CAR MODEL WITH TRANSFER FUNCTION AGAINST QUARTER CAR MODEL IN VIRTUAL WIND TUNNEL (REAL); GRAPHICAL COMPARISON

That is the principal objective and conclusion; to compare the quarter car model wit and without aerodynamic TF.

If the difference is low, the procedure will be correct and acceptable; for that, it work with a geometry model, with a new configuration:

The same values as point 4, but another incidence angle and span (Fig.49 and 50):

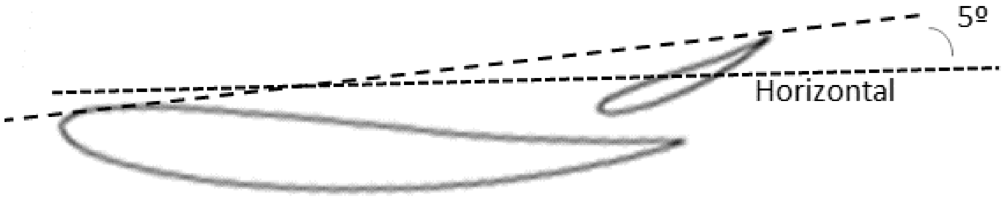

Fig.49: Incidence angle.

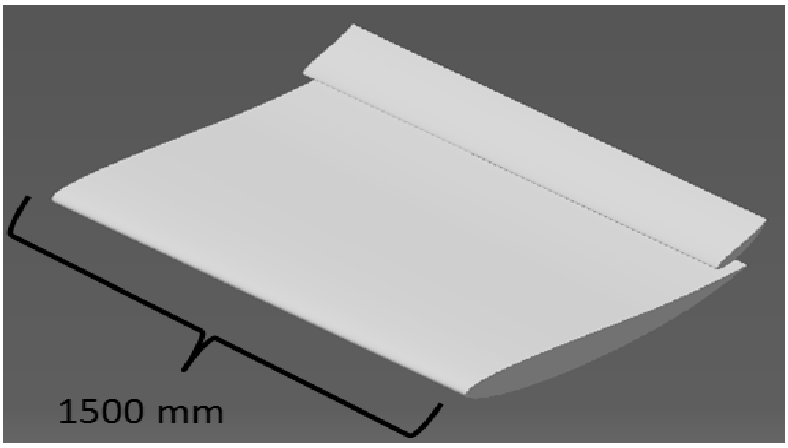

Fig.50. Span geometry.

The values in virtual wind tunnel, against quarter car without aero and aero model Transfer Function, are (sprung and unsprung mass) (Fig.51 and 52):

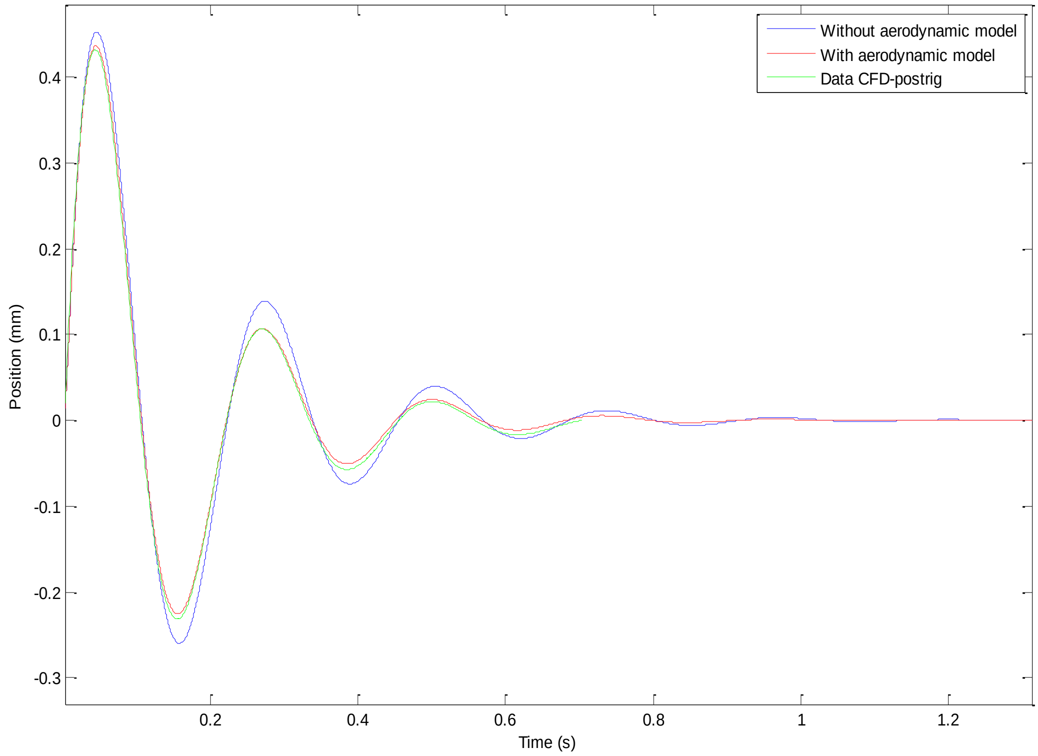

Fig.51: Displacement sprung, without aero, with aero and CFD test.

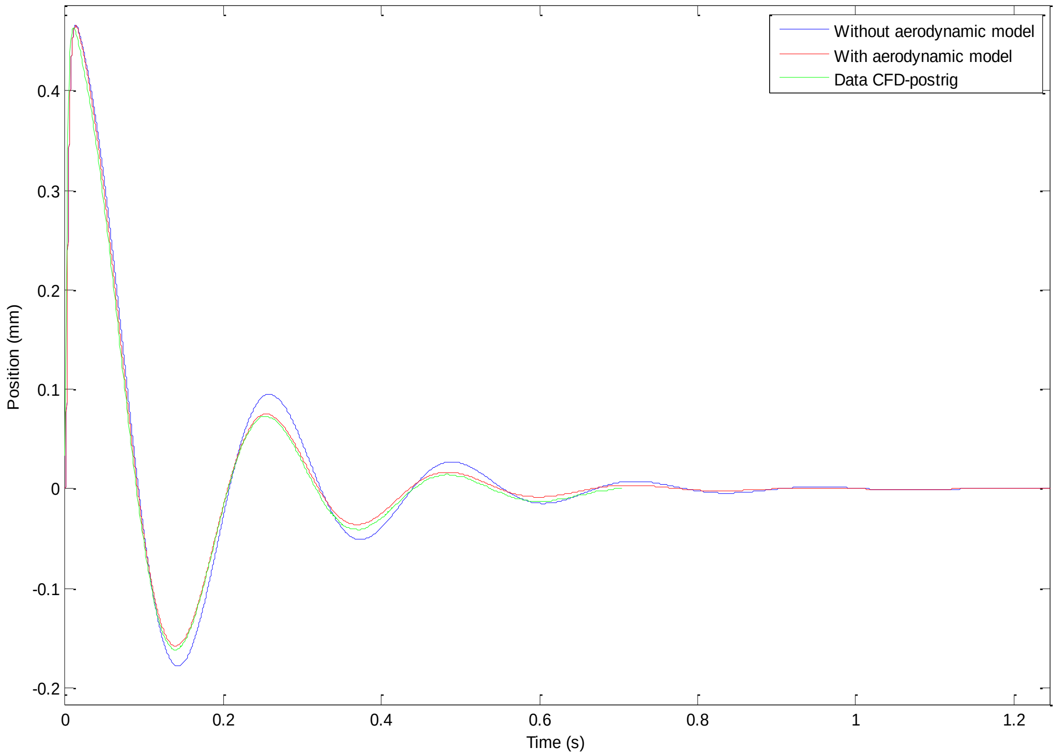

Fig.52: Displacement unsprung, without aero, with aero and CFD test.

Details of Fig.51 and 52 (Fig.53 and 54):

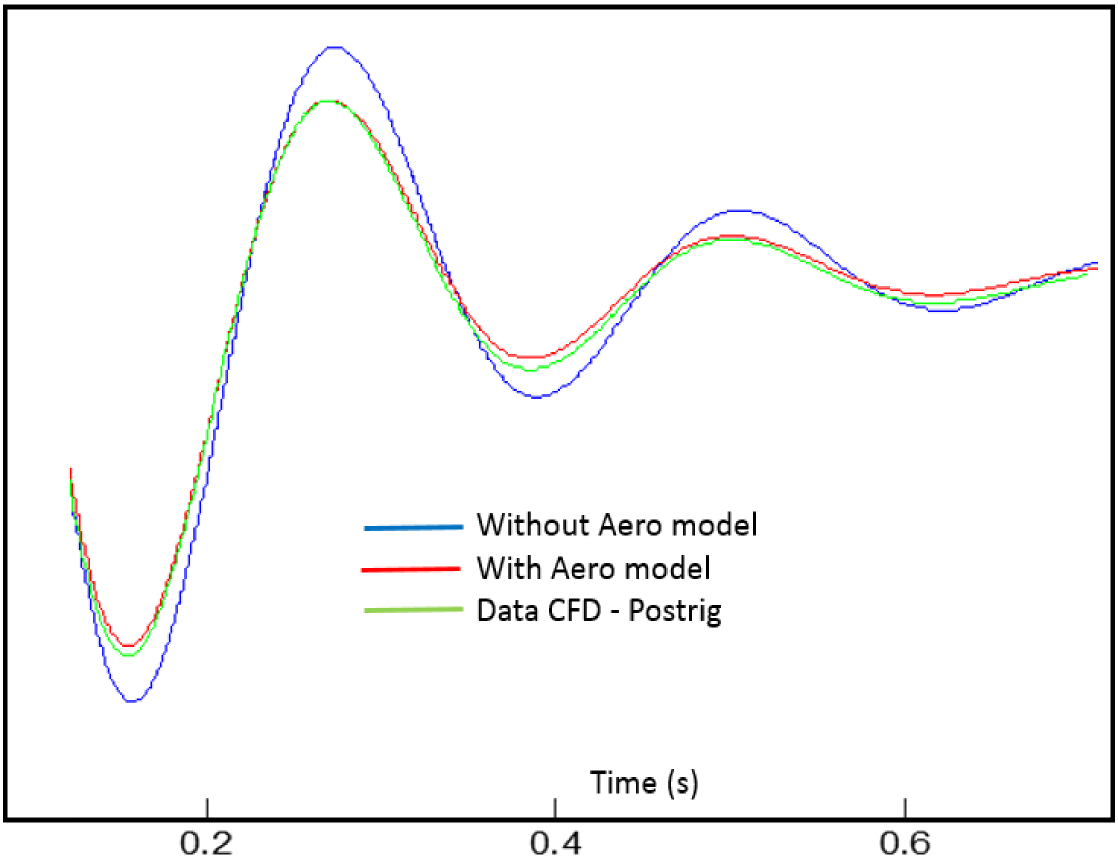

Fig.53: Detail of Fig.51

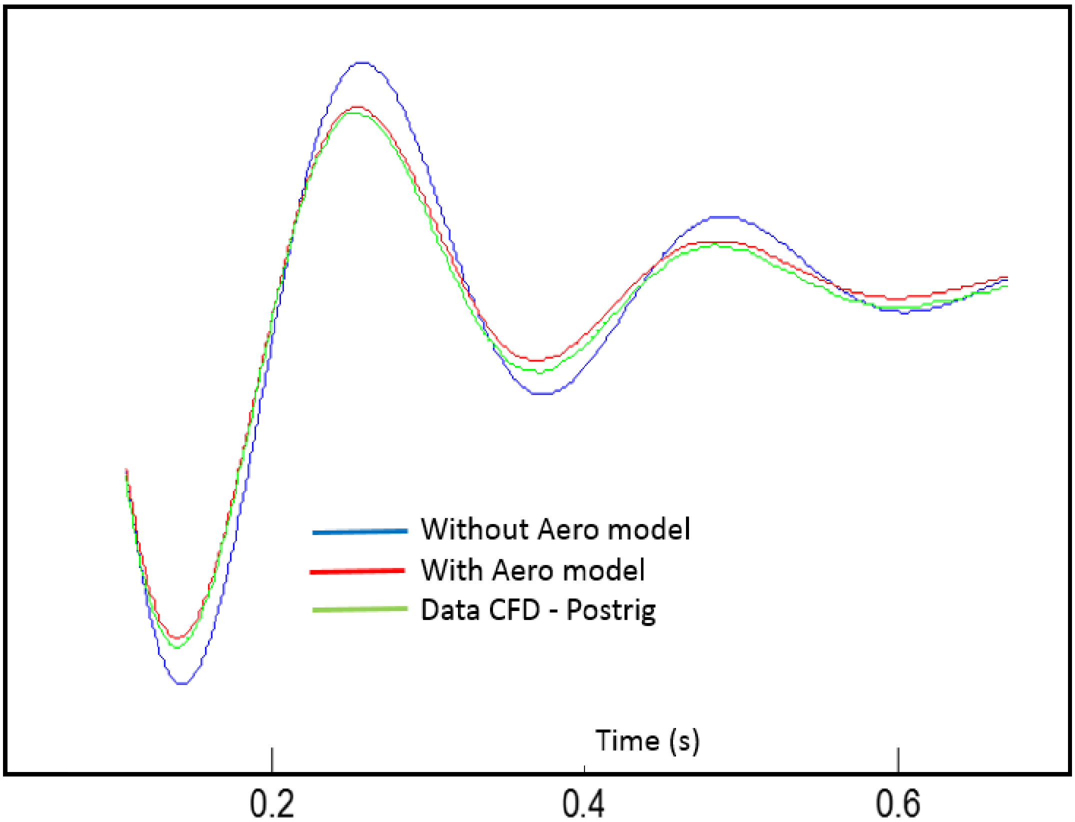

Fig.54: Detail of Fig.52

The difference between wind tunnel virtual values and quarter car model with TF is very little; perhaps the difference between wind tunnel virtual values and quarter car model without aerodynamics, is big; all that is good for validating the new procedure and analysis.

The bode plot of quarter car model (sprung and unsprung mass) is (Fig.55 and 56):

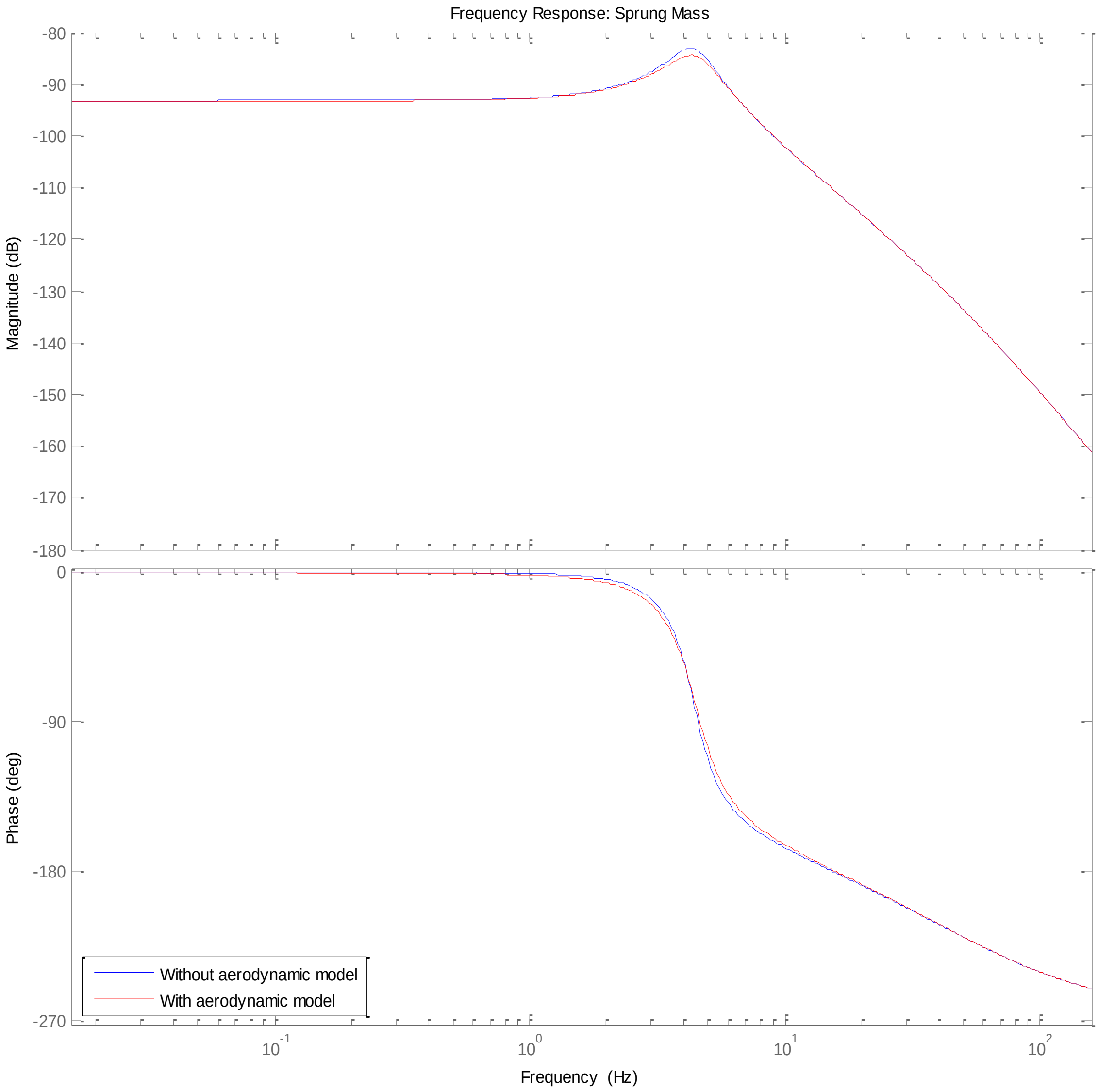

Fig.55: Sprung mass bode plot.

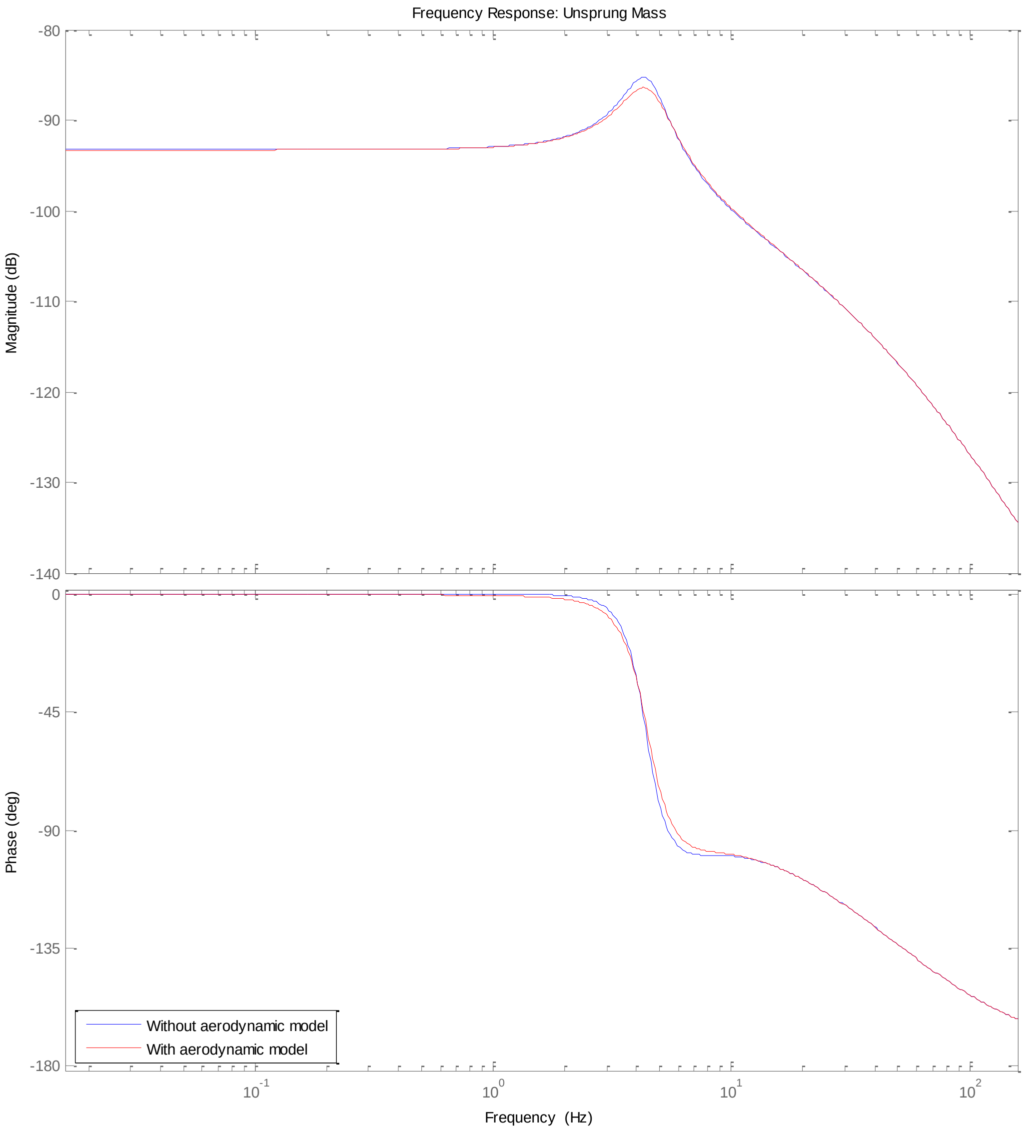

Fig.56: Unsprung mass bode plot.

It can see that the gain is lower, so the attenuation is lower too.

6. NUMERIC COMPARISON: OPTIMIZING SUSPENSION: PERFORMANCE INDEX

The goal is improve the suspension and so, the behavior car in the track; in order to avoid that, needless to express a value for improving:

- High Contact patch load.
- Constant contact patch load.
- Littles variations of sprung mass height; constant heights.

In a race car, is very important the aerodynamic behavior; that is; the parameters most important in a race car, are the pitch and the ride height; so is very important that this parameters will be constant (Fig.57):

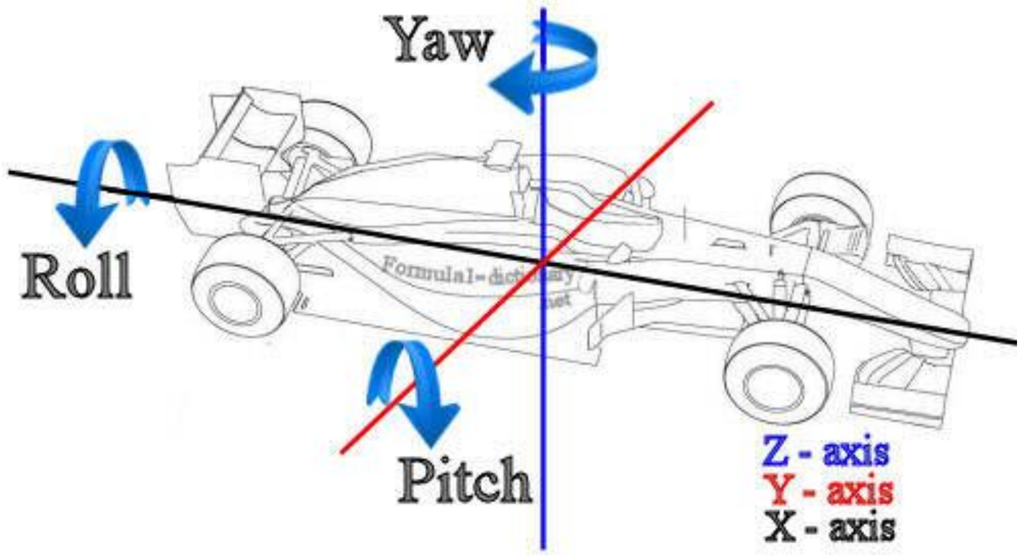

Fig.57: Car freedom degrees / movements in every axes; Ride heights.

For that, in a quarter car model, it is also important to maintain the constant height of the sprung mass.

Show below a set of values Performances Index “PI”:

6.1. DEFINITION PI_1

This method is based on studying the Bode plot (Fig.58), and so, minimize the resonance peak:

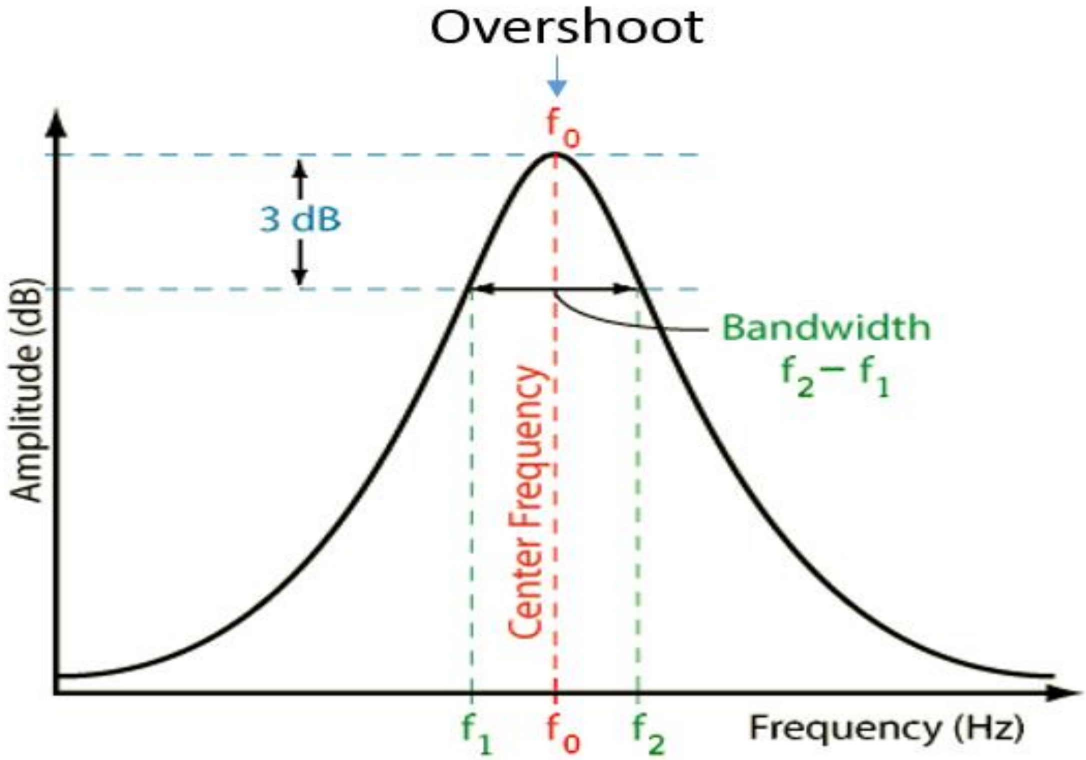

Fig.58: Overshoot and bandwidth.

The Eq.8 is a first Performance Index definition:

$$PI_1 = \frac{OVERSHOOT}{BANDWIDTH}$$

Eq.8: Performance Index PI_1

In order to improve the unsprung mass behavior (to optimize the contact patch load (so the grip) and maintain its constants), is necessary to reduce the overshoot and augment the bandwidth (the response will be quickly); the same for sprung mass; for that (Table 4):

↗ Increase Reduce ↘

	Unsprung mass		Sprung mass	
	Overshoot	Bandwidth	Overshoot	Bandwidth
Tyre constant	↗	↗	↘	↗
Suspension constant	↘	↗	↗	↗
Tyre Damper	↗	↗	↗	↗
Suspension damper			↗	
Sprung mass	↘		↗	↗

Table 4: What doing to reduce the PI_1

6.2. DEFINITION PI_2

In order to improve the damper or suspension in general, also exists a Performance Index (PI_2) (Eq.9), including the body vertical vibration acceleration, the suspension dynamic travel and the tire vibration (N = number points):

$$PI_2 = \lim_{N \to \infty} \frac{1}{N} \int_0^N \left[q_1 (y_2 - y_3)^2 + q_2 (y_1 - y_2)^2 + q_3 \ddot{y}_1^2 \right]$$

Eq.9: Definition PI_2

The symbols q1, q2 and q3, represent the weight coefficients of every variable, depending if the goal is improve the comfort passage or have a sport driving. In this study, the principal goal is to reduce the tire vibration and reduce the variation height of chassis in order to have the aero constant, because the tire degradation will be less and the downforce will be more constant; for that, q3=0. Another parameter very important for improving the car behavior, is that the contact patch between tire and track, always exist and with the contact patch load greater possible.

6.3. DEFINITION PI_3

The contact load and so a good contact between track and tires, depend the patch tire; the tire have a deformation in function of a lot parameters:

- Pressure inflate.
- Load.
- Geometry setup (camber, toe, tire dimensions, etc….).
- Speed rotation.

Is very important to know what this deformation is and so, the contact patch and the contact patch load.

Let the area contact patch "Ac"; it possible to define the next performance index PI_3 in two forms (Eq.10 and 11):

$$PI_{3a} = \frac{PI_1}{Ac}$$

Eq.10: Performance Index PI_3 with PI_1

$$PI_{3b} = \frac{PI_2}{Ac}$$

Eq.11: Performance Index PI_3 with PI_2

In this way, is possible to improve the damper behavior if PI_3 is lower.

7. APPLICATION REAL: IMPROVE SUSPENSION PARAMETERS

It work about values from Table 3; the goal is improve the setup; from a damper and spring suspension data, it tested a values between 150% up and 50'% down; that is: from 1600 N/ms (damper), it tested values between 2400 N/ms and 800 N/ms; the same with spring.

7.1. PI_1

For the base setup (Table 3), the bode plot is: (Fig.59):

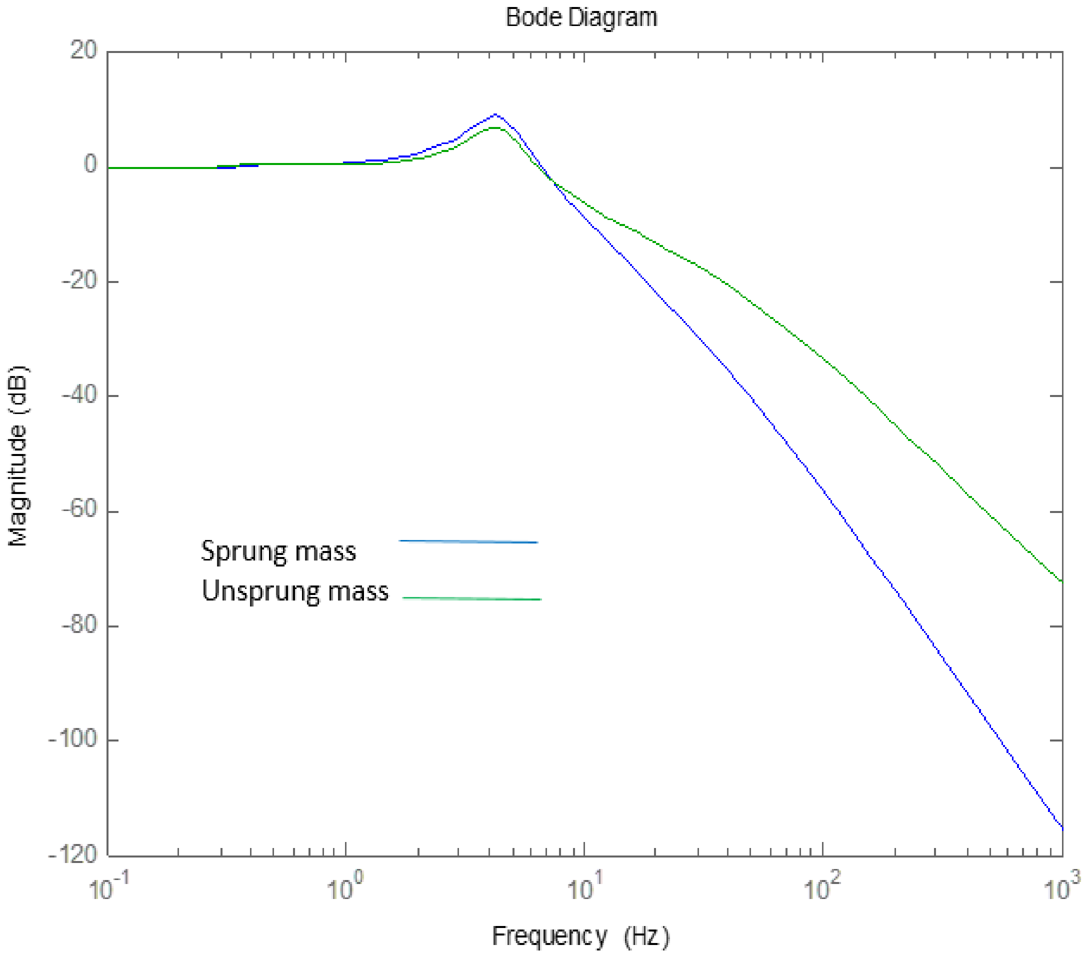

Fig.59: Bode Plot setup base from Table 3, to improve.

The blue color mean that the PI_1 is lower; red is greater; it show the performance index for sprung and unsprung mass (Fig.60 and 61):

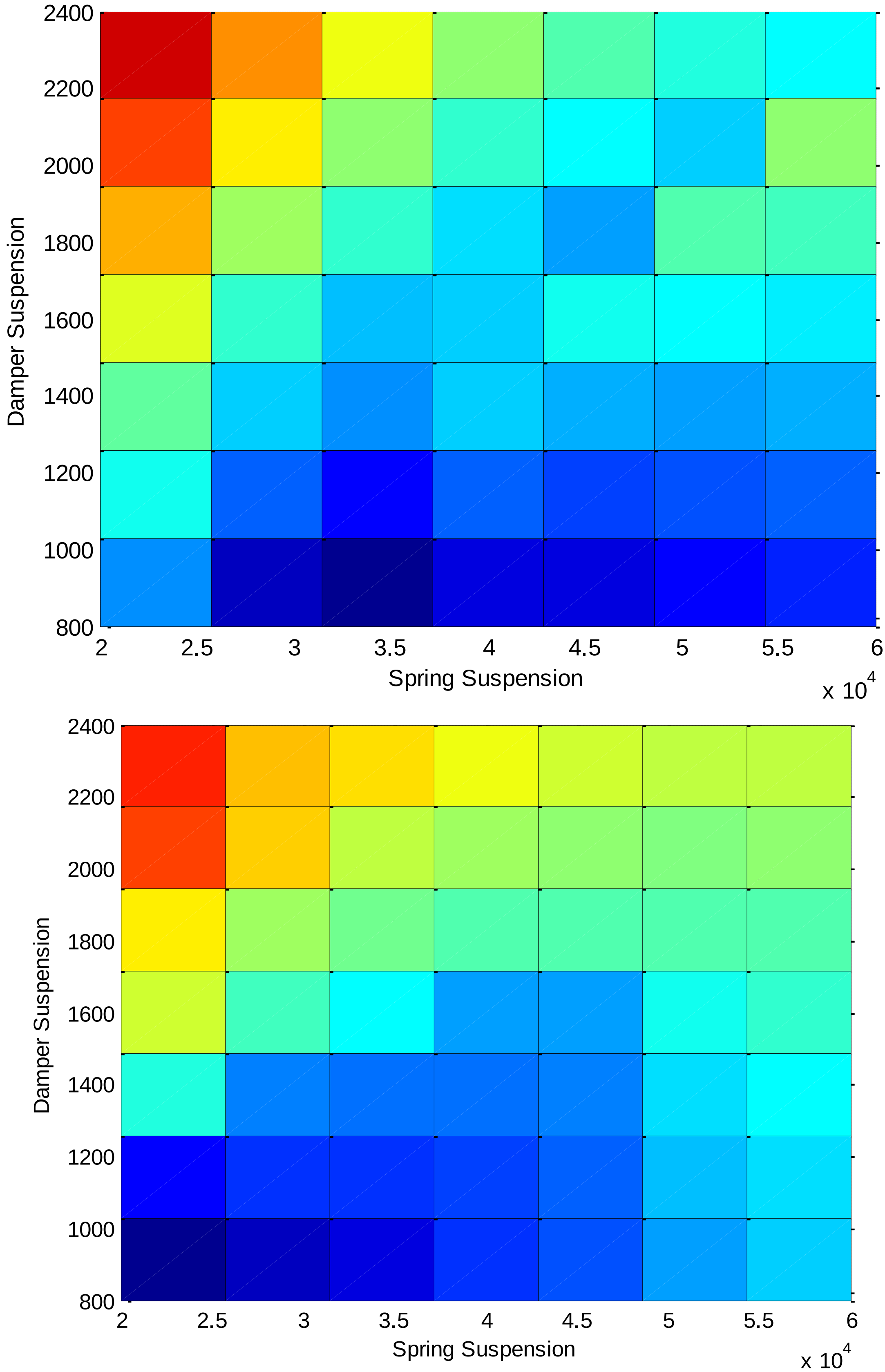

Fig.60: PI_1 Sprung mass.

Fig.61: PI_1 Unsprung mass.

Showing the results, is possible to improve the damper and spring:

The both zones blue is around spring value 30.000 N/m and Damper value 800 N/ms; improve both values, is complicate because areas blue are not the same. So is necessary as always, a compromise between damper and spring.

7.2. PI_2

In this case, it work about improve the suspension parameters (only damper) for a step; it work with 1 track irregularity-step (Fig.62):

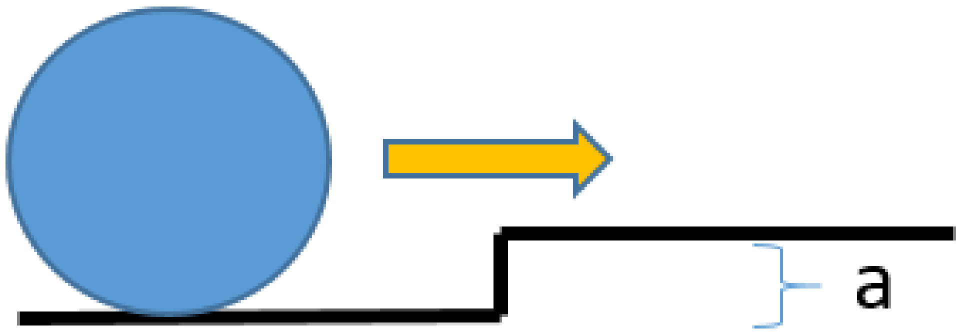

Fig.62: Step test profile.

Test values:

a= 0.01 m, and Speed= 50 m/s; the quarter car values are Table 3.

The test interval for improving the suspension damper is (800 N/ms, 2400 N/ms). It will work also, with the contact path and the contact patch load; in order to calculate the contact or not of a tire, if the tire deflection (spring tire) is greater than initial tire thickness, there is not contact; that is the contact condition. The results are (Table 4):

	Performace Index - PI_2		
	Sprung Mass	Unsprung Mass	Full
Damper Suspension			
800 N/ms	229,1942	145,4842	187,3392
1000 N/ms	202,5659	136,0461	169,3060
1200 N/ms	185,9747	132,0770	159,0259
1400 N/ms	175,9793	131,7866	153,8830
1600 N/ms	170,6357	134,0474	152,3416
1800 N/ms	168,7428	138,1440	153,4434
2000 N/ms	169,4451	143,5712	156,5082
2200 N/ms	172,0971	149,9598	161,0285
2400 N/ms	176,1739	157,0183	166,5961

Table 4: PI_2 with aerodynamic TF, and different Damper suspension.

Representing in lines Fig.63:

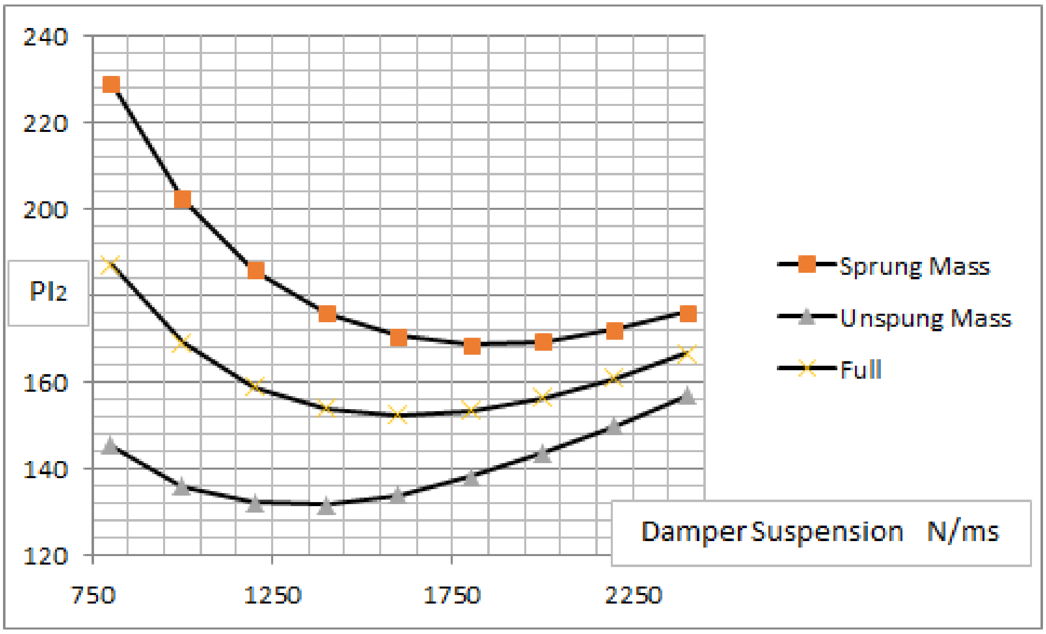

Fig.63: Lines of PI_2 (Table 4).

There are some thinks very important about:

- The damper optimum for sprung mass is around 1760 N/ms. This value is ideal in car with big aerodynamic influence: Formula 1 for example.
- The damper optimum for unsprung mass is around 1300 N/ms; that value is ideal in car with aerodynamic not very important:

rally car for example. Also, there will be a high conservation of tires.
- The damper optimum for full suspension is around 1530 N/ms.
- For 2400 N/ms there is the bigger contact patch load.

These conclusions about the PI_2 results, are very important because is possible already to know really the car behavior and so, improve exactly the damper or suspension parameters in general.

8. ACKNOWLEDGEMENTS

The author would like to acknowledge the support of my family.

9. CONCLUSIONS AND FUTURE DIRECTIONS

In this paper presents the study of the influence of a double wing profile in the dynamic behavior of a model of a quarter of a vehicle suspension. First, there have been experiments virtual wind tunnel (using techniques CFD), to obtain a transfer function of the double profile representing the behavioral model of downforce when the wing varies its vertical position (movement heave).

To obtain have introduced different position sinusoidal signals at different frequencies and there have been variations in the amplitude and phase shift downforce.

Simulations with different amplitudes of position shows that the transfer function is unchanged if the first cycle of the sinusoidal signal over time is taken. However, when registering more than one cycle of the sinusoidal signal a shift in the time position of the gap between observed and downforce for any frequency. In the module variations are observed.

This illustrates the nonlinear nature of the system. In order to simplify the study of the problem applied to the dynamic model of a quarter vehicle suspension, it has chosen to use a transfer function of the aerodynamics of the double profile built considering the first cycle of the sinusoidal signal in time.

When the behavior of a model of a quarter of a vehicle suspension are compared with and without the double transfer function profile shows that the airfoil has an effect of reducing the amplitude of the temporal fluctuations and a slight reduction in speed of these oscillations. From the viewpoint of frequency response results in a lower resonance peak and a slight reduction in bandwidth of both the sprung mass and the unsprung. This entails taking into account the aerodynamic model if it is to optimize the behavior of the suspension. Simulations for optimizing suspension performance by applying different rates of return show that the results are different as note or aerodynamic model. In addition, it is noted that in any case has to reach a compromise between the behavior of the sprung mass and the unsprung.

In the future it is expected to deepen in several respects. For one, it will be a more detailed phase variations of the transfer function study aerodynamics are taken into account when more than one time cycle sinusoidal position signal. Furthermore, we will study how the effect soil affects the aerodynamic transfer function different profiles. The ultimate goal is to study the effects of aerodynamics on a model of bike and full car model; in these cases, will be necessary study the pitch and heave variations.

Finally, another application will be improve the comfort of passengers in bus, or vehicle transport in general.

10. REFERENCES

[1] J.Molina and X.Zhang, “On the unsteady motion and stability of a Heaving Airfoil in Ground Effect,” AIAA J., vol. 49, no. 6, pp. 1168–1179, Apr. 2011.
[2] Steven L.Brunton, Clarence W. Rowley, "Modeling the unsteady aerodynamic forces on small-scale wings", Princeton University, Princeton, NJ 08544, AIAA 2009-1127, January 2009.
[3] S.Y.Chenga,b, M.Tsubokura, T.Nakashimac, Y.Okada and T.Nouzawa, "Numerical quantification of aerodynamic damping on pitching of vehicle inspired bluff body", Hokkaido University.
[4] Chang-kwon Kang, Yeon Sik Baik, Luis Bernal, Michael V. Ol, and Wei Shyy, "Fluid Dynamics of Pitching and Plunging Airfoils of Reynolds Number between 1×104 and 6×104", 47th AIAA Aerospace Sciences Meeting Including The New Horizons Forum and Aerospace Exposition 5 - 8 January 2009, Orlando, Florida.
[5] Leonardo Tavares Stutz, Fernando Alves Rochinha, "Synthesis of a Magneto-Rheological vehicle suspension system built on the variable structure control approach", Technical papers dynamics, vibrations and acoustics.

[6] Mark Lowenberg, Hilton Kyle, "Derivation of unsteady aerodynamic models from wind tunnel multi-axis test rigs", ICAS 2002 Congress.
[7] Steven L.Brunton, Clarence W.Rowley, "Low-dimensional state-space representations for classical unsteady aerodynamic models", Princeton University, Princeton, NJ 08544.
[8] Henri Kowalczyk, "Damper Tuning with the use of a Seven Post Shaker Rig", ARC Indianapolis-Reynard Motorsport, SAE technical papers 2002-01-0804.
[9] Basileios Mavroudakis, Peter Eberhard, "Mode decoupling in vehicle suspensions applied to race cars", III European Conference on Computational Mechanics Solids, Structures and Coupled Problems in Engineering C.A. Mota Soares et.al. (eds) Lisbon, Portugal, 5–8 June 2006.
[10] Abdolvahab Agharkakli, Ghobad Shafiei Sabet, Armin Barouz, "Simulation and Analysis of Passive and Active Suspension System Using Quarter Car Model for Different Road Profile", International Journal of Engineering Trends and Technology- Volume3 Issue5-2012.
[11] Claudiu Valentin Suciu, Tsubasa Tobiishi, and Ryouta Mouri, "Modeling and Simulation of a Vehicle Suspension with Variable Damping versus the Excitation Frequency", Department of intelligent mechanical engineering Fukuoka institute of technology Fukuoka - Japan.
[12] Steven Roy, Zhaoheng Liu, "Road vehicle suspension and performance evaluation using a two dimensional vehicle model".
[13] I.A.Craighead, "Sensing tyre pressure, damper condition and wheel balance from vibration measurements", Department of Mechanical Engineering, University of Strathclyde.
[14] Scott Floyd and E.Harry Law, "Simulation and Analysis of Suspension and Aerodynamic Interactions of Race Cars", Clernson University.
[15] Unkoo Lee, "A proposition for new vehicle dynamic performance index", Journal of Mechanical Science and Technology 23 (2009) 889~893.
[16] A.G.Thompson, "The effect of damping on the performance of vibration absorbers in an active suspension", Journal of Sound and Vibration (1989) 133(3), 457-465.
[17] Luis P.Bernal, "Unsteady Force Measurements in Pitching-Plunging Airfoils", 39th AIAA Fluid Dynamics Conference 22 - 25 June 2009, San Antonio, Texas.
[18] Patrick C.Murphy, Vladislav Klein, "Estimation of aircraft unsteady aerodynamic parameters from dynamic wind tunnel testing", AIAA-2001-4016,
[19] N.Moore, Professor P.A.Wilson, A.J.Peters, "An investigation into wing ground effect airfoil geometry", School of Engineering Sciences, University of Southampton, SO17 1BJ, UK.

[20] G. Verros, S. Natsiavas, "Design Optimization of Quarter-car Models with Passive and Semi-active Suspensions under Random Road Excitation", Department of Mechanical Engineering, Aristotle University, 54 124 Thessaloniki, Greece, Department of Mechanical and Industrial Engineering, University of Thessaly, 38 334 Volos,Greece.
[21] Anil ShirahattiI, P.S.S. Prasad, Pravin Panzade, M.M. Kulkarni, "Optimal design of passenger car suspension for ride and road holding".
[22] Matteo Corno, Stefano Bottelli, Mara Tanelli, Cristiano Spelta, Sergio M. Savaresi, "Active Control of Aerodynamic Surfaces for Ride Control in Sport Vehicles", Preprints of the 19th World Congress The International Federation of Automatic ControlCape Town, South Africa. August 24-29, 2014.
[23] Jorge Hurel Ezetaa, Anthony Mandowb, Alfonso García Cerezo, "Los Sistemas de Suspensión Activa y Semiactiva:Una Revisión, Revista Iberoamericana de Automática e Informática industrial 10 (2013) 121–132.
[24] Malcolm C.Smith, and Fu-Cheng Wang, "Performance Benets in Passive Vehicle Suspensions Employing Inerters".
[25] Mohammad Reza Tabeshpour, A.Akbar Golafshani, "The Effect of Added Mass Fluctuation on HeaveVibration of TLP", Researchgate papers, Available from: A. Akbar Golafshani Retrieved on: 24 June 2015.
[26] Supavut Chantranuwathana1 and Huei Peng, "Adaptive robust force control for vehicle active suspensions", INTERNATIONAL JOURNAL OF ADAPTIVE CONTROL AND SIGNAL PROCESSING Int. J. Adapt. Control Signal Process. 2004; 18:83–102 (DOI: 10.1002/acs.783).
[27] M.Corno, S.Bottelli, G.Panzani, M.Tanelli, C.Spelta, S.M.Savaresi, "Improving High Speed Road-Holding Using Actively Controlled Aerodynamic Surfaces", July 17-19, 2013, Zürich, Switzerland.
[28] Dinçer Özcan, Ümit Sönmez, and Levent Güven, "Optimisation of the Nonlinear Suspension Characteristics of a Light Commercial Vehicle", Hindawi Publishing Corporation International Journal of Vehicular Technology Volume 2013, Article ID 562424, 16 pages.
[29] Jose Daniel Pardo Barcelo, "Optimisation of Racing Car Suspensions featuring Inerters", The Department of Mechanical Engineering and Mathematical Sciences Oxford Brookes University 2012.
[30] Hiroyuki Sawamoto, Tsuyoshi Yasuki, Hiroshi Tanaka, Kazuyoshi Ishii, "Unsteady aerodynamic analysis around oscillating Ahmed body by LS-Dyna ver.980", Toyota Motor corporation, 9th European LS.Dyna conference 2013.
[31] R. Aiguabella, “Formula One Rear Wing Optimization”, UPC Barcelona, 2011.

[32] M. Ariff, S. M. Salim, and S. C. Cheah, "Wall Y + Approach for dealing with Turbulent Flow over a Surface mounted cube : Part 2 – High Reynolds Number," Seventh International Conference on CFD in the Minerals and Process Industriesnd Process Industries, 2009.
[33] T. Cebeci, J. P. Shao, F. Kafyeke, and E. Laurendeau, "Computational fluid dynamics for engineers: from panel to Navier-Stokes methods with computer programs," 2005.
[34] I. A. Craighead, "Sensing tyre pressure, damper condition and wheel balance from vibration measurements", Department of Mechanical Engineering, University of Strathclyde.